Chapter 18

Neutrino Mixing and Oscillations

18.1 Introduction

Neutrino oscillation is purely a quantum mechanical phenomenon, in which a neutrino of one flavor, say ν_α develops a component of a neutrino of another flavor, say ν_β, where $\alpha, \beta = e, \mu, \tau$, and $\alpha \neq \beta$. This phenomenon of neutrino oscillation implies that neutrinos have definite mass and their flavor eigenstates are different from their mass eigenstates.

The idea of neutrino masses, mixing, and oscillations was first proposed in 1957–58 [179] just after the two-component neutrino theory was confirmed by the Goldhaber et al. [153] experiment. Pontecorvo [179] conjectured the idea of neutral particle (not necessarily being elementary particle) oscillation based on the analogy with kaon regeneration (K^0–$\bar{K}^0$ oscillation), and argued that : 'If the two- component neutrino theory should turn out to be incorrect (which at present seems to be rather improbable) and if the conservation law of neutrino charge would not apply, then in principle neutrino $\leftrightarrow$ antineutrino transitions could take place in vacu'. At that time only one type of neutrino existed, therefore, for the two-component theory, there were only left-handed neutrinos ν_L and right-handed antineutrinos $\bar{\nu}_R$, implying oscillations between ν_L and $\bar{\nu}_R$. These transitions are however not possible because of the conservation of total angular momentum.

Around the same time, Davis [968] conducted an experiment using reactor antineutrino beams and looked for the electron in the reaction

$$\bar{\nu}_e + {}^{37}_{17}\mathrm{Cl} \rightarrow e^- + {}^{37}_{18}\mathrm{Ar}, \tag{18.1}$$

which showed negative results. Contrary to the negative observations, a rumor reached Pontecorvo that Davis has observed the aforementioned event before the actual publication of the work. Based on the assumed positive results, in 1958, Pontecorvo, in an another paper [969], concluded that: "The result of the Davis experiment was nonzero probability for the process under study, if confirmed, definitely shows that the (strict) law of neutrino charge conservation

https://doi.org/10.1017/9781108489065.019 Published online by Cambridge University Press

is not valid." He suggested that the events could be due to the transitions $\bar{\nu}_R \to \nu_R$. However, this explanation contradicted the two-component neutrino theory, where only the left-handed neutrinos (ν_L) or the right-handed antineutrinos $(\bar{\nu}_R)$ participate in the weak interaction. Therefore, the suggestion of ν_R and similarly, $\bar{\nu}_L$ by Pontecorvo implies the existence of a class of neutrinos which are noninteracting; they are called sterile neutrinos.

Based on this argument, he suggested that for non-identical ν and $\bar{\nu}$, the following processes should be observed in nuclei:

$$p \to n + \beta^+ + \nu\,, \quad n \to p + \beta^- + \bar{\nu}, \tag{18.2}$$

while if the strict law of neutrino charge conservation is not valid, then the following processes should be observed:

$$p \to n + \beta^+ + \bar{\nu}\,, \quad n \to p + \beta^- + \nu. \tag{18.3}$$

In 1962, Maki, Nakagawa, and Sakata introduced the mixing of two neutrinos [71] by contemplating that: "It should be stressed at this stage that the definition of the particle state of neutrino is quite arbitrary; we can speak of 'neutrinos' which are different from weak neutrinos but expressed by the linear combinations of the latter. We assume that there exists a representation which defines the 'true neutrinos' through some orthogonal transformation applied to the representation of weak neutrinos:

$$\begin{aligned} \nu_1 &= \nu_e \cos\delta + \nu_\mu \sin\delta, \\ \nu_2 &= -\nu_e \sin\delta + \nu_\mu \cos\delta, \end{aligned}$$

where δ is a real constant."

In 1967, when the two flavors of neutrinos ν_e and ν_μ were proved to exist, Pontecorvo [970] in a paper reiterated that: "If leptonic charge is not an exactly conserved quantum number (and in this case, the neutrino mass would be different from zero), then oscillations of the type $\bar{\nu} \leftrightarrow \nu$, $\nu_\mu \leftrightarrow \nu_e$, which are similar to oscillations in a beam of K^0 mesons become possible for neutrino beams." This paper also discussed the observation of such a possibility through solar neutrino oscillations and the following conclusions were made: "From the point of view of detection possibilities, an ideal object is the sun. If the oscillation length is much smaller than the radius of the solar region which effectively produces neutrinos which will give the main contribution to the experiments which are being planned now...." Few years later, Davis et al. [971, 972] confirmed that the detected flux of solar neutrinos was about 2–3 times smaller than the theoretically predicted flux by Bahcall [973, 182] in the standard solar model. For the solar neutrino problem, the prediction made by Pontecorvo was naturally accepted. Apart from the solar neutrinos, for the atmospheric neutrinos, the atmospheric neutrino flux was expected to be in the ratio 2 : 1 for ν_μ and ν_e type neutrinos because of the following reactions:

$$\begin{aligned} \pi^\pm &\longrightarrow \mu^\pm + \nu_\mu(\bar{\nu}_\mu), \\ \mu^\pm &\longrightarrow e^\pm + \nu_e(\bar{\nu}_e) + \bar{\nu}_\mu(\nu_\mu). \end{aligned}$$

https://doi.org/10.1017/9781108489065.019 Published online by Cambridge University Press

The observations on atmospheric neutrinos later showed that there exists a discrepancy between the observed flux and the predicted flux; this discrepancy in the flux is known as the atmospheric neutrino anomaly. The ratio $\frac{(\nu_\mu+\bar{\nu}_\mu)}{(\nu_e+\bar{\nu}_e)}$ deviates from the predicted flux 2 : 1, which was possible only if neutrinos could oscillate from one flavor to another. A similar anomaly was seen in the region of very low energy with reactor antineutrinos [974, 975] when the precise energy spectrum of antineutrinos emitted from the fission of ^{235}U, ^{239}Pu, ^{238}U, and ^{241}Pu were calculated [976, 977], and compared with the experimentally observed spectrum [978].

Experimentally, the discovery of the neutrino oscillations was confirmed through the observation of atmospheric neutrinos in Kamiokande [898, 901, 902], SOUDAN [979], Super-Kamiokande [903, 980], solar neutrinos at Super-K [981, 982, 983, 984], SAGE [985], BOREXino [986, 987], Gallex/GNO [988], SNO [989] and reactor antineutrinos at KamLAND [978], Daya Bay [990], RENO [991], and Double Chooz [992, 993]. Moreover, the accelerator experiments like K2K [994], MiniBooNE [995], NOMAD [996], CHORUS [997], MINOS [998, 999], T2K [1000, 1001], NOvA [1002, 1003, 628, 1004], OPERA [119, 1005, 1006, 1007, 1008], etc. also confirmed the phenomenon of neutrino oscillation. In fact, acknowledging the efforts made to understand neutrino oscillation physics, the Nobel prize in Physics for the year 2015 was awarded jointly to T. Kajita "for the discovery of atmospheric neutrino oscillations" and A. McDonald "for the discovery of neutrino oscillations in the solar sector".

In this chapter, we are going to study neutrino oscillations in vacuum in two- and three-flavor scenarios and obtain the expression of survival probability (chances of neutrinos of a particular flavor to keep the same identity) and transition probability (the probability of neutrinos oscillating from one flavor to another). Then, we shall discuss the effect of the interaction of neutrinos with matter on the neutrino oscillation probability. This is known as the Mikheyev–Smirnov–Wolfenstein (MSW) effect after the scientists Mikheyev, Smirnov, and Wolfenstein [1009, 1010]; it enhances the neutrino oscillation probability. Finally, we shall discuss in brief, the sensitivity of the different experiments toward the determination of oscillation parameters and conclude the chapter with a discussion on sterile neutrinos.

18.2 Neutrino Mixing

18.2.1 Two-flavor neutrino oscillations in vacuum

The oscillation of neutrino from one flavor to another is only possible when the neutrino mass eigenstates (or propagation states), say ν_1 and ν_2, are different from the flavor states, say ν_α and ν_β, where $\alpha, \beta = e, \mu$ or for any two neutrino flavors among e, μ, and τ. This implies that the quantized neutrino field of a definite flavor does not coincide with the quantized neutrino field that has definite mass. In fact, a given flavor state ν_α is expressed as an orthonormal linear combination of mass eigenstates ν_i, $i = 1, 2$ with mass m_i, such that

$$|\nu_\alpha\rangle = \sum_{j=1}^{2} U_{\alpha j}|\nu_j\rangle, \tag{18.4}$$

https://doi.org/10.1017/9781108489065.019 Published online by Cambridge University Press

where $U_{\alpha j}$ is a 2×2 unitary matrix ($U^\dagger = U^{-1}$) and is generally expressed as:

$$\hat{U} = \begin{bmatrix} U_{e1} & U_{e2} \\ U_{\mu 1} & U_{\mu 2} \end{bmatrix} \quad , \quad \hat{U}^\dagger = \begin{bmatrix} U^*_{e1} & U^*_{\mu 1} \\ U^*_{e2} & U^*_{\mu 2} \end{bmatrix}, \text{ such that } \hat{U}\hat{U}^\dagger = \begin{bmatrix} 1 & 0 \\ 0 & 1 \end{bmatrix}. \quad (18.5)$$

Similarly, the mass eigenstates in terms of flavor eigenstates may be expressed as:

$$|\nu_j\rangle = \sum_\alpha (U^\dagger)_{j\alpha} \, |\nu_\alpha\rangle = \sum_\alpha U^*_{\alpha j} \, |\nu_\alpha\rangle. \quad (18.6)$$

Since a 2×2 unitary matrix U is real, $U^*_{\alpha j} = U_{\alpha j}$ and

$$|\bar{\nu}_\alpha\rangle = U^*_{\alpha j} \, |\bar{\nu}_j\rangle = U_{\alpha j} \, |\bar{\nu}_j\rangle, \quad (18.7)$$

where $|\bar{\nu}_j\rangle$ ($|\bar{\nu}_\alpha\rangle$) are the mass (flavor) eigenstates of an antineutrino. This implies that:

$$\sum_\alpha U_{\alpha j} \, U^*_{\alpha k} \quad = \quad \delta_{jk} \quad \text{and} \quad \sum_j U_{\alpha j} \, U^*_{\beta j} = \delta_{\alpha\beta}. \quad (18.8)$$

Since a 2×2 matrix is parameterized in terms of one real parameter say θ, we may write:

$$\begin{bmatrix} \nu_e \\ \nu_\mu \end{bmatrix} = \begin{bmatrix} \cos\theta & \sin\theta \\ -\sin\theta & \cos\theta \end{bmatrix} \begin{bmatrix} \nu_1 \\ \nu_2 \end{bmatrix} = U \begin{bmatrix} \nu_1 \\ \nu_2 \end{bmatrix}, \quad (18.9)$$

where θ is the neutrino mixing angle. This means that the definite flavor eigenstates of neutrinos ν_e and ν_μ are composed exclusively of the mass eigenstates ν_1 and ν_2. The oscillation matrix is chosen to be unitary because in a scenario of two ν flavors in nature, where one flavor of neutrino (say ν_e) oscillates to another flavor (say ν_μ) and vice versa, there is no loss in total neutrino flux implying that the total probability of oscillation (including all possible cases) is unity, that is,

$$P(\nu_e \to \nu_e) \; + \; P(\nu_e \to \nu_\mu) \quad = \quad P(\nu_\mu \to \nu_\mu) \; + \; P(\nu_\mu \to \nu_e) = 1. \quad (18.10)$$

We demonstrate the oscillation probability in a two-flavor scenario, in vacuum, in Figure 18.1. Suppose we start with a π^+decay at rest (at point A in Figure 18.1(i)), which gives rise to l^+_α and ν_α. The detector is placed at B and we observe ν_α through charged current interactions giving rise to a charged lepton of flavor α, that is, l^-_α. Now if we observe the same flavour of charged leptons produced at the detector site B as the flavour of ν_αs that were there at the production site A, then that means no oscillation has taken place. However, if at B, we find charged lepton(s) of a different flavor, say β that means among the ν_αs, while traveling toward the detector, a few have got converted into another flavor ν_β whose interaction at the detector site B has given rise to a different lepton l^-_β (Figure 18.1(ii)). The oscillation of neutrinos of one flavor to another flavor is only possible when the propagation states (say ν_1 and ν_2) are different from the flavor states (say ν_α and ν_β), where ν_α is some linear combination of ν_1 and ν_2, while ν_β is some different linear combination of ν_1 and ν_2.

https://doi.org/10.1017/9781108489065.019 Published online by Cambridge University Press

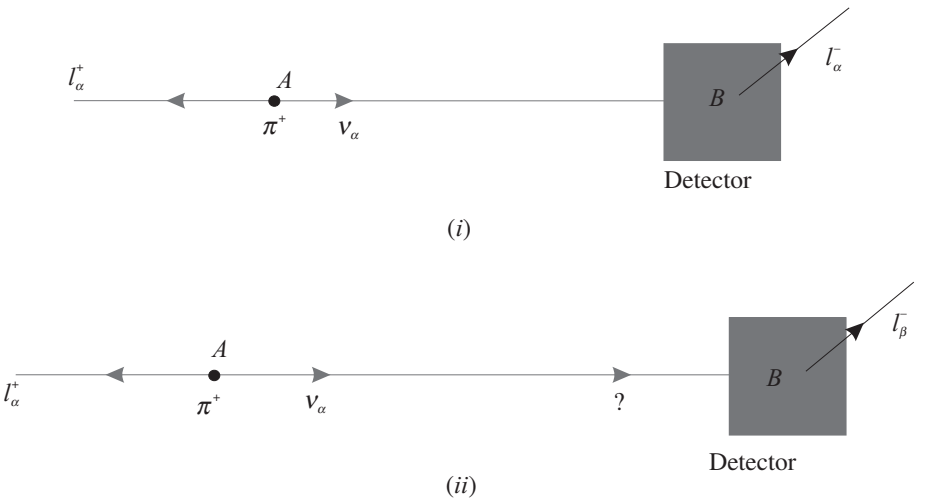

Figure 18.1 The top figure represents a no oscillation case where at "A", ν_αs are produced along with l_α^+ and travel a short distance, and at "B", the same number of l_α^- are detected through charged current interactions (ν_α, l_α^-). The bottom figure represents an oscillation case, where at "A", ν_αs are produced along with l_α^+ and travel some distance, and at "B", some of the charged leptons of flavor l_β^- are observed which is only possible when on the way, a few ν_α get converted into ν_β.

To calculate the oscillation probability in a two-flavor oscillation scenario, we start with time evolution equation for a neutrino of definite flavor α (ν_e or ν_μ) by using the Schrödinger equation

$$i\frac{\partial|\nu_\alpha(t)\rangle}{\partial t} = H\,|\nu_\alpha(t)\rangle, \tag{18.11}$$

where H, for the evolution of states in vacuum is a free Hamiltonian and its solution would be

$$|\nu_\alpha(t)\rangle = e^{-iHt}|\nu_\alpha(t=0)\rangle = e^{-iEt}|\nu_\alpha(t=0)\rangle, \tag{18.12}$$

where $|\nu_\alpha(t=0)\rangle$ or $|\nu_\alpha(0)\rangle$ is the state at the initial time $t=0$. Now to start with, if we have ν_e beam, then

$$|\nu_\alpha(0)\rangle = |\nu_\alpha(t=0)\rangle = |\nu_e\rangle. \tag{18.13}$$

Since neutrino mass eigenstates are defined by $|\nu_j\rangle$,

$$H|\nu_j\rangle \;=\; E_j|\nu_j\rangle\;;\;\; j=1,2, \quad \text{and} \quad E_j = \sqrt{|\vec{p}_j|^2 + m_j^2} \tag{18.14}$$

$$\Rightarrow \;\; |\nu_\alpha(t)\rangle \;=\; \sum_{j=1}^{2} e^{-iE_jt}\,U_{\alpha j}|\nu_j\rangle. \tag{18.15}$$

https://doi.org/10.1017/9781108489065.019 Published online by Cambridge University Press

Let us say that a neutrino of generation α after a time interval t is given by the eigenstate $|\nu_\alpha, t\rangle$, such that

$$|\nu_\alpha, t\rangle = \sum_{j=1}^{2} U_{\alpha j}\, |\nu_j, t\rangle = \sum_{j=1}^{2} U_{\alpha j}\, |\nu_j, 0\rangle\, e^{-iE_j t} \tag{18.16}$$

$$= \sum_{j=1}^{2} U_{\alpha j}\, e^{-iE_j t} \left(\sum_{\beta} U^*_{\beta j} |\nu_\beta, 0\rangle \right). \tag{18.17}$$

Survival probability, that is, the probability that a neutrino that had started ($t = 0$) with a flavor α remains ν_α, is obtained by using amplitude defined as:

$$\mathcal{M}_{\alpha\alpha}(t) = \langle \nu_\alpha, 0 | \nu_\alpha, t\rangle = \delta_{\alpha\beta} \sum_{j=1}^{2} U_{\alpha j}\, e^{-iE_j t} U^*_{\beta j} = \sum_{j=1}^{2} U_{\alpha j}\, e^{-iE_j t} U^*_{\alpha j}, \tag{18.18}$$

where $\sum_\beta \langle \nu_\alpha(0) | \nu_\beta(0)\rangle = \delta_{\alpha\beta}$ and the survival probability

$$P_{(\nu_\alpha \to \nu_\alpha)}(t) = |\mathcal{M}_{\alpha\alpha}(t)|^2 = |\sum_{j=1}^{2} U_{\alpha j}\, e^{-iE_j t} U^*_{\alpha j}|^2. \tag{18.19}$$

Similarly, transition probability, that is, the probability that a neutrino that has started ($t = 0$) with a flavor α oscillates into another flavor ν_β, is given by:

$$P_{(\nu_\alpha \to \nu_\beta)}(t) = |\mathcal{M}_{\alpha\beta}(t)|^2 = |\sum_{j=1}^{2} U_{\alpha j}\, e^{-iE_j t} U^*_{\beta j}|^2. \tag{18.20}$$

Similarly, for antineutrinos in the two-flavor scenario, the transition probability is given by:

$$P_{(\bar{\nu}_\alpha \to \bar{\nu}_\beta)}(t) = |\mathcal{M}_{\alpha\beta}(t)|^2 = |\sum_{j=1}^{2} U^*_{\alpha j}\, e^{-iE_j t} U_{\beta j}|^2,$$

$$= |\sum_{j=1}^{2} U_{\alpha j}\, e^{-iE_j t} U^*_{\beta j}|^2 = P_{(\nu_\alpha \to \nu_\beta)}(t). \tag{18.21}$$

Suppose that a neutrino is produced with a definite energy E regardless of which ν_j it happens to be. Then for a particular mass eigenstate ν_j, it has momentum

$$p_j = \sqrt{E^2 - m_j^2} \approx E - \frac{m_j^2}{2E}. \tag{18.22}$$

We find

$$\mathcal{M}(\nu_j \text{ propagates}) \approx e^{-i\frac{m_j^2}{2E}L} \approx e^{-i\frac{m_j^2}{2p}L}. \tag{18.23}$$

Since highly relativistic neutrinos have $E \approx p$, the propagation amplitudes in both the cases are approximately equal.

https://doi.org/10.1017/9781108489065.019 Published online by Cambridge University Press

Using Eq. (18.23) in Eq. (18.20), the probability of oscillation from one flavor to other flavor may be obtained as:

$$\begin{aligned} P(\nu_e \to \nu_\mu) &= \left| \sum_{j=1}^{2} U_{ej} e^{-i\frac{m_j^2 t}{2E}} U_{\mu j}^* \right|^2 \\ &= |U_{e1}|^2 |U_{\mu 1}|^2 + |U_{e2}|^2 |U_{\mu 2}|^2 + U_{e1} U_{\mu 1}^* U_{e2}^* U_{\mu 2} e^{i\frac{m_2^2 t}{2E}} e^{-i\frac{m_1^2 t}{2E}} \\ &\quad + U_{e1}^* U_{\mu 1} U_{e2} U_{\mu 2}^* e^{-i\frac{m_2^2 t}{2E}} e^{i\frac{m_1^2 t}{2E}}. \end{aligned}$$

Using U from Eq. (18.9), we may write

$$\begin{aligned} P(\nu_e \to \nu_\mu) &= 2\cos^2\theta \sin^2\theta - 2\cos^2\theta \sin^2\theta \left(\frac{e^{i\frac{(m_2^2 - m_1^2)t}{2E}} + e^{-i\frac{(m_2^2 - m_1^2)t}{2E}}}{2} \right) \\ &= \sin^2(2\theta) \sin^2\left(\frac{\Delta m^2 L}{4E} \right), \end{aligned} \tag{18.24}$$

using $\Delta m^2 = m_2^2 - m_1^2$, $t = L/c = L$ ($c = 1$ in natural units). Therefore, from Eq. (18.24), it may be observed that in the two-flavor case, only $\sin^2 2\theta$ and Δm^2 are responsible for transitions between neutrinos of two different flavors for a fixed energy E and length L. The same expression will hold good for the antineutrinos, that is, $P(\nu_e \to \nu_\mu) = P(\bar{\nu}_e \to \bar{\nu}_\mu)$. Furthermore, the probability of transition between the two-flavor states would be the same for $\nu_\alpha \to \nu_\beta$ and $\nu_\beta \to \nu_\alpha$, that is,

$$P(\nu_\mu \to \nu_e) = P(\nu_e \to \nu_\mu)\ . \tag{18.25}$$

Therefore,

$$P(\nu_e \to \nu_\mu) = P(\nu_\mu \to \nu_e) = P(\bar{\nu}_e \to \bar{\nu}_\mu) = P(\bar{\nu}_\mu \to \bar{\nu}_e),$$

and in fact, it will be true for any two flavors among the three different flavors of neutrinos.

For a definite L, the oscillation probability will vary with E. Therefore, a proper choice of L corresponding to the range of E ensures proper sensitivity to the oscillation probability. The quantity in the parenthesis of Eq. (18.24) is dimensionless and is evaluated numerically by inserting appropriate factors of $\hbar$ and c, that is,

$$\Delta m^2 \frac{L}{4E} = \frac{(\Delta m c^2)^2 L/c}{4E\hbar} = \frac{\Delta m^2 c^4}{\text{eV}^2} \frac{L}{\text{km}} \frac{\text{GeV}}{E} \left[\frac{\text{eV}^2\ \text{km}}{4\text{GeV}\ (\hbar c)} \right]. \tag{18.26}$$

If Δm, L, and E are measured in eV, km, and GeV, respectively and $\hbar c = 0.197396$ GeV-fm, then this relation is expressed as:

$$1.267 \Delta m^2(\text{eV}^2) \frac{L(\text{km})}{E(\text{GeV})}.$$

https://doi.org/10.1017/9781108489065.019 Published online by Cambridge University Press

Equation (18.24) can also be written in terms of oscillation length as:

$$P(\nu_e \to \nu_\mu) \quad = \tfrac{1}{2}\sin^2(2\theta)(1-\cos 2\pi \tfrac{L}{L_{\text{osc}}}), \tag{18.27}$$

where

$$L_{\text{osc}} \quad = \tfrac{4\pi E}{\Delta m^2} = 4\pi\hbar c \tfrac{E}{\Delta m^2} \simeq 2.48 \tfrac{\frac{E}{\text{GeV}}}{\frac{\Delta m^2}{\text{eV}^2}} \text{km}. \tag{18.28}$$

Neutrino oscillation length L_{osc} should be either equal to or less than the source to detector distance otherwise the oscillations will not be developed. Thus, the quantity that determines whether oscillation has occurred or not when neutrinos of a particular flavor have traveled a distance between the source and the detector is given by:

$$\frac{\pi L}{L_{\text{osc}}} = \frac{L\Delta m^2}{4E} = 1.267 \frac{\left(\frac{\Delta m^2}{\text{eV}^2}\frac{L}{\text{km}}\right)}{\left(\frac{E}{\text{GeV}}\right)}.$$

In Figure 18.2, we have plotted the survival probability $P(\nu_\alpha \to \nu_\alpha)$ vs. $\frac{\Delta m^2}{4}\frac{L}{E}$ curve for $\sin^2 2\theta_{12} = 0.83$, where it may be observed that:

- if the detector is very close to the neutrino source, that is, $L << L_{\text{osc}}$ leading to $\frac{L}{E} << \frac{1}{\Delta m^2}$, there will be no oscillation (Figure 18.2(a)).
- the most sensitive region to observe oscillation is $\frac{L}{E} \gtrsim \frac{1}{\Delta m^2}$. This region is said to be the necessary condition for the oscillation (Figure 18.2(b)).
- for $L >> L_{\text{osc}}$, several oscillations will occur and the average of the oscillation probabilities would be the most acceptable measurement (Figure 18.2(c)).

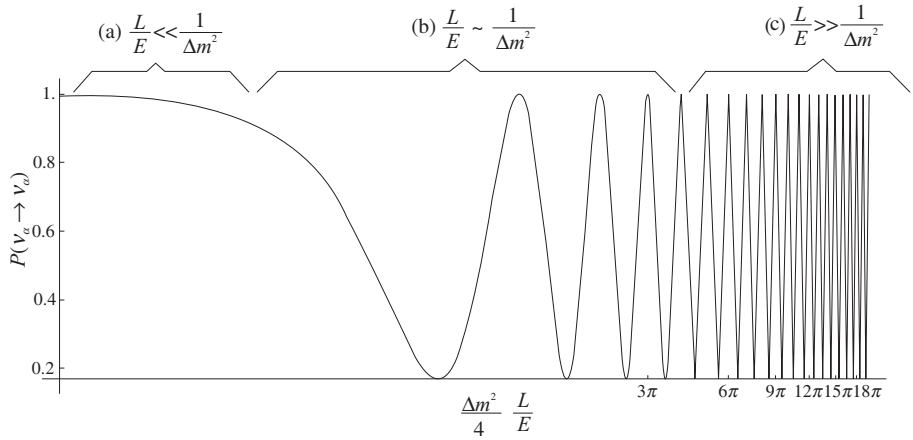

Figure 18.2 Oscillation probability vs. $\frac{\Delta m^2}{4}\frac{L}{E}$ curve for $\sin^2 2\theta = 0.83$. (a) shows no oscillation scenario in the region $\frac{1}{\Delta m^2} >> \frac{L}{E}$; (b) shows the threshold condition for oscillation at $\frac{1}{\Delta m^2} \sim \frac{L}{E}$ and (c) shows the oscillation scenario in the region $\frac{1}{\Delta m^2} << \frac{L}{E}$.

https://doi.org/10.1017/9781108489065.019 Published online by Cambridge University Press

The survival probability $P(\nu_\alpha \to \nu_\alpha)$, that is, the probability of a neutrino ν_α of flavor, say $\alpha = e$ or μ retaining its original flavor, is given by:

$$\begin{aligned} P(\nu_\alpha \to \nu_\alpha) &= 1 - P(\nu_\alpha \to \nu_{\beta\neq\alpha}) \\ &= 1 - \sin^2(2\theta)\sin^2\left(1.267\,\Delta m^2(\text{eV}^2)\frac{L(\text{km})}{E(\text{GeV})}\right). \end{aligned} \tag{18.29}$$

Thus, the transition probability $P(\nu_\alpha \to \nu_\beta)$, that is, the probability of a neutrino ν_α of flavor, say $\alpha = e$ changing into another flavor β, say ν_μ, is given by:

$$\begin{aligned} P(\nu_\alpha \to \nu_\beta) &= P(\nu_\alpha \to \nu_{\beta\neq\alpha}) \\ &= \sin^2(2\theta)\sin^2\left(1.267\,\Delta m^2(\text{eV}^2)\frac{L(\text{km})}{E(\text{GeV})}\right). \end{aligned} \tag{18.30}$$

The survival probability is measured by the disappearance channel, that is, we measure the fraction of neutrinos of the original flavor left. On the other hand, the transition probability is measured by the appearance channel, that is, we measure the fraction of neutrinos of new flavor.

The different parameters used to describe the neutrino oscillation phenomenon are as follows:

i) **The mixing angle θ:** This is one of the two fundamental parameters of neutrino oscillation phenomenology. Notice that if $\theta = 0$, the flavor eigenstates are identical to the mass eigenstates, that is, a ν_α will propagate from the source to the detector as ν_α. If $\theta = \frac{\pi}{4}$, then the oscillations are said to be maximal and at some point along the path between the source and the detector, all of the neutrinos of one flavor (say α) will oscillate to another flavor (say β). A nonzero value of θ signifies how much the flavor eigenstates are different from the mass eigenstates.

ii) **The mass squared difference** Δm^2: This is another fundamental parameter of neutrino oscillations. It governs the frequency of oscillations. For a two-flavor neutrino oscillation, there will be two mass eigenstates and $\Delta m^2_{12} = m_1^2 - m_2^2$. For oscillation to ocuur, either one of the neutrino mass eigenstate should be nonzero or the two mass eigenstates should be nonzero and non-degenerate. Since the probability of oscillation would be unchanged for $\Delta m^2_{21} \to -\Delta m^2_{12}$, it does not tell whether $m_1 > m_2$ or vice versa.

iii) **L/E**: The transition probability (Eq. (18.30)) depends periodically on the quantity L/E and describes neutrino oscillation. The L/E ratio is the parameter which is in the control of experimentalists for accelerator or reactor experiments, where L is the distance between the source and the detector, and E is the energy of the neutrino. Equation (18.30) implies that the oscillation becomes maximum for

$$1.267\Delta m^2\frac{L}{E} = (2n+1)\frac{\pi}{2} \;\Rightarrow \Delta m^2\frac{L}{E} > 1, \quad \text{where } n = 0, 1, 2... \tag{18.31}$$

or

$$\frac{L}{E} = (2n+1)\frac{\pi}{2.534\Delta m^2}.$$

https://doi.org/10.1017/9781108489065.019 Published online by Cambridge University Press

For example, if we take $n = 0$ (corresponding to the first oscillation maxima), $\Delta m^2 = 2.5 \times 10^{-3}\text{eV}^2$ and $L = 500$ km, 1000 km, and 2000 km, the first maxima should be observed respectively at the energies $E = 1.01$ GeV, 2.02 GeV, and 4.04 GeV, which can be clearly seen from the plots shown in Figure 18.3. It may be observed that for $E < 500\text{MeV}$ and $\frac{L}{E} \gg \frac{1}{\Delta m^2}$, the average of the oscillation probability would be the most acceptable measurement.

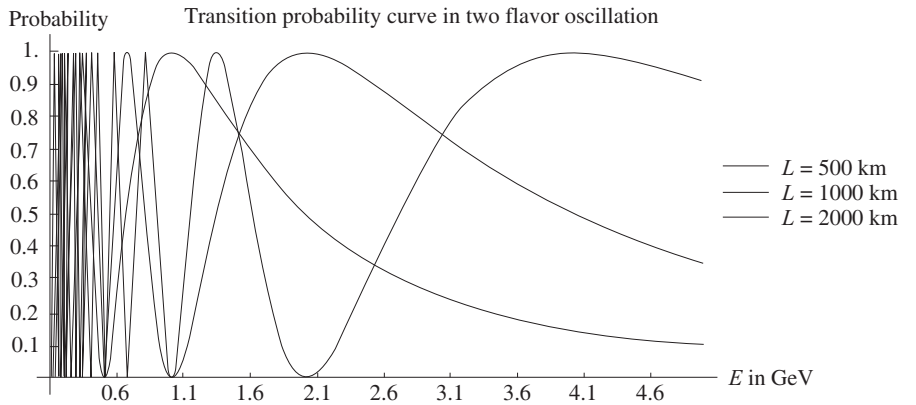

Figure 18.3 Transition probability curve for two-flavor neutrino oscillations for different values of L.

iv) The frequency of oscillation is controlled by Δm^2 and is shown in Figure 18.4, which is obtained using Eq. (18.30) for a constant L and θ. This figure is a plot of the transition probability as a function of neutrino energy (0.1 GeV to 5 GeV) at constant $L = 2000$ km and $\theta = 45^\circ$, for the several values of Δm^2 viz., $\Delta m^2 = 2.2 \times 10^{-3}\text{eV}^2$, 2.5×10^{-3} eV^2 and 2.8×10^{-3} eV^2. It may be observed that Δm^2 is directly proportional to E, that is, with the increase in Δm^2, the probability curve gets shifted toward the higher energies.

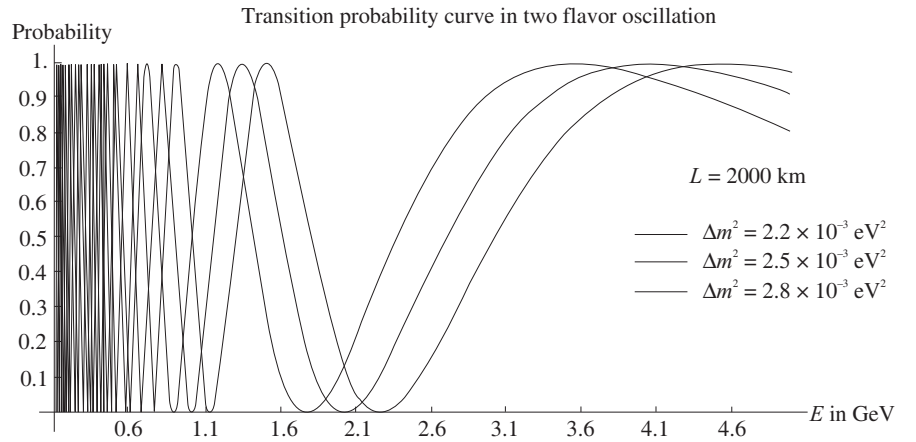

Figure 18.4 Transition probability curve for two-flavor neutrino oscillations for different values of Δm^2.

https://doi.org/10.1017/9781108489065.019 Published online by Cambridge University Press

v) In Figure 18.5, we have plotted transition probability $P(\nu_\alpha \to \nu_\beta)$ for the two values of energy $E = 1$ GeV and 3 GeV, using $\Delta m^2 = 2.5 \times 10^{-3}$ and $\sin^2(2\theta)$=1. The peak occurs at the oscillation length $L^{\text{osc}} = 992$ km and 2976 km respectively which can be seen from Figure 18.5. It may be observed that at some distance from the source L, all the neutrinos of one flavor are converted into the other flavor, whereas at some other length, there is no oscillation, while at other values of L, we have a mixture of ν_e and ν_μ. It can also be observed from this figure that the transition probability depends significantly upon neutrino energy, that is, the oscillation probability is not the same for the two different energies.

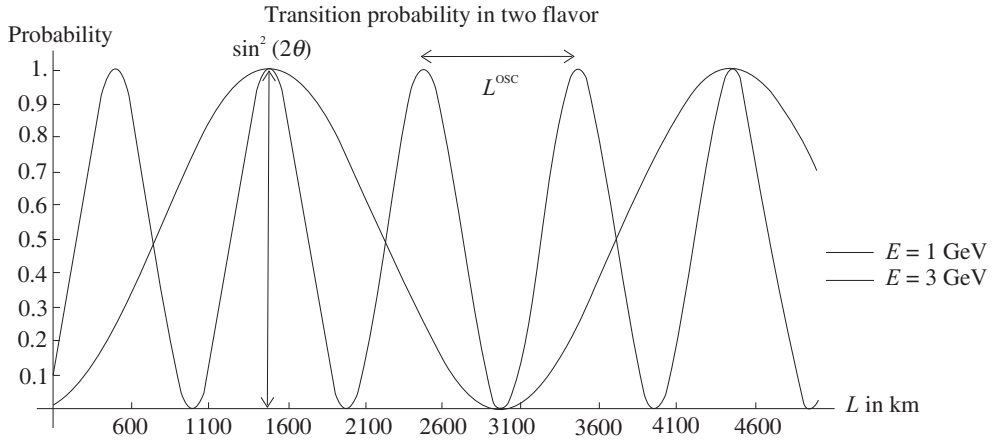

Figure 18.5 L^{osc} curves obtained using Eq. (18.30) at E_ν=1 GeV and 3 GeV, for $\Delta m^2 = 2.5 \times 10^{-3}\text{eV}^2$ and $\sin^2(2\theta)$=1.

18.2.2 Three-flavor neutrino oscillation in vacuum

The three-flavor neutrinos, viz., ν_e, ν_μ, ν_τ, while propagating in space, travel as some admixture of three neutrino mass eigenstates, viz., ν_i $(i = 1, 2, 3)$ with masses m_i, which are related by a 3×3 unitary matrix

$$|\nu_\alpha\rangle = \sum_{i=1}^{3} U_{\alpha i} |\nu_i\rangle \quad (\alpha = e, \mu, \tau)\,. \tag{18.32}$$

$$\begin{pmatrix} \nu_e \\ \nu_\mu \\ \nu_\tau \end{pmatrix} = \begin{pmatrix} U_{e1} & U_{e2} & U_{e3} \\ U_{\mu 1} & U_{\mu 2} & U_{\mu 3} \\ U_{\tau 1} & U_{\tau 2} & U_{\tau 3} \end{pmatrix} \begin{pmatrix} \nu_1 \\ \nu_2 \\ \nu_3 \end{pmatrix}. \tag{18.33}$$

To conserve the total flux of neutrinos, the total probability of oscillation in a three-flavor scheme is given by:

$$P(\nu_e \to \nu_e) + P(\nu_e \to \nu_\mu) + P(\nu_e \to \nu_\tau) = 1. \tag{18.34}$$

https://doi.org/10.1017/9781108489065.019 Published online by Cambridge University Press

This probability is obtained for the other flavors in a similar manner. If the neutrinos are Dirac particles, then the neutrino mixing matrix is similar to the quark mixing matrix in both the number of mixing angles and CP phase as discussed in Chapter 6. Consequently, the lepton mixing matrix U is given by the Pontecorvo–Maki–Nakagawa–Sakata [179, 71] (PMNS) mixing matrix as:

$$U = \begin{pmatrix} 1 & 0 & 0 \\ 0 & c_{23} & s_{23} \\ 0 & -s_{23} & c_{23} \end{pmatrix} \begin{pmatrix} c_{13} & 0 & s_{13}e^{-i\delta} \\ 0 & 1 & 0 \\ -s_{13}e^{i\delta} & 0 & c_{13} \end{pmatrix} \begin{pmatrix} c_{21} & s_{12} & 0 \\ -s_{12} & c_{12} & 0 \\ 0 & 0 & 1 \end{pmatrix} \tag{18.35}$$

$$= \begin{pmatrix} c_{12}c_{13} & s_{12}c_{13} & s_{13}e^{-i\delta} \\ -s_{12}c_{23} - c_{12}s_{13}s_{23}e^{i\delta} & c_{12}c_{23} - s_{12}s_{13}s_{23}e^{i\delta} & c_{13}s_{23} \\ s_{12}s_{23} - c_{12}s_{13}c_{23}e^{i\delta} & -c_{12}s_{23} - s_{12}s_{13}c_{23}e^{i\delta} & c_{13}c_{23} \end{pmatrix}, \tag{18.36}$$

where $s_{ij} = \sin\theta_{ij}$ and $c_{ij} = \cos\theta_{ij} (i, j = 1, 2, 3)$. In this parameterization of the mixing matrix, the mixing parameters can take values in the ranges $0 \leq \theta_{ij} \leq \frac{\pi}{2}$ $(i, j = 1, 3; i \neq j)$; a $\delta \neq 0, \pi$ would lead to CP violation. The parameters of the matrix are determined in oscillation experiments. The values of δ different from 0 and π imply CP violation in neutrino oscillations in vacuum [1011, 1012, 1013].

Following the same procedure as used in the case of two-flavor neutrino oscillation, we write the oscillation amplitude for the oscillation from flavor α to flavor β as:

$$\mathcal{M}(\nu_\alpha \longrightarrow \nu_\beta) = \sum_i U_{\alpha i} e^{-i\frac{m_i^2}{2E}t} U^*_{\beta i},$$

which leads to the oscillation probability given by:

$$P(\nu_\alpha \longrightarrow \nu_\beta) = \left|\mathcal{M}(\nu_\alpha \longrightarrow \nu_\beta)\right|^2 = \sum_{i=1}^{3}\sum_j U_{\alpha i} U^*_{\beta i} U^*_{\alpha j} U_{\beta j} e^{i\frac{L}{2E}(m_j^2 - m_i^2)}. \tag{18.37}$$

The transition probability $P(\nu_\alpha \longrightarrow \nu_\beta)$ may be written as:

$$P(\nu_\alpha \longrightarrow \nu_\beta) = \sum_{i=j} U^*_{\alpha i} U_{\beta i} U_{\alpha j} U^*_{\beta j} + \sum_{i\neq j} U^*_{\alpha i} U_{\beta i} U_{\alpha j} U^*_{\beta j} - 2\sum_{i\neq j} U^*_{\alpha i} U_{\beta i} U_{\alpha j} U^*_{\beta j} \times \sin^2\left(\frac{L\Delta m^2_{ji}}{4E}\right) + i\sum_{i\neq j} U^*_{\alpha i} U_{\beta i} U_{\alpha j} U^*_{\beta j} \sin\left(\frac{L\Delta m^2_{ji}}{2E}\right) \tag{18.38}$$

which is evaluated by first taking the first and second terms and writing:

$$P_1 + P_2 = \sum_i\sum_j U^*_{\alpha i} U_{\beta i} U_{\alpha j} U^*_{\beta j} = \left|\sum_i U_{\alpha i} U^*_{\beta i}\right|^2 = \begin{cases} 1 & \text{for } \alpha = \beta, \\ 0 & \text{otherwise.} \end{cases} \tag{18.39}$$

https://doi.org/10.1017/9781108489065.019 Published online by Cambridge University Press

Now taking the third term of Eq. (18.38),

$$\begin{aligned} P_3 &= -2\sum_{i\neq j} U^*_{\alpha i}U_{\beta i}U_{\alpha j}U^*_{\beta j}\sin^2\left(\frac{L\Delta m^2_{ji}}{4E}\right) \\ &= -2\left\{\sum_{i>j} U^*_{\alpha i}U_{\beta i}U_{\alpha j}U^*_{\beta j}\sin^2\left(\frac{L\Delta m^2_{ij}}{4E}\right) + \sum_{i<j} U^*_{\alpha i}U_{\beta i}U_{\alpha j}U^*_{\beta j}\sin^2\left(\frac{L\Delta m^2_{ji}}{4E}\right)\right\} \\ &= -2\left\{\sum_{i>j}\sin^2\left(\frac{L\Delta m^2_{ij}}{4E}\right)\left[\left(U^*_{\alpha i}U_{\beta i}U_{\alpha j}U^*_{\beta j}\right) + \left(U^*_{\alpha i}U_{\beta i}U_{\alpha j}U^*_{\beta j}\right)^*\right]\right\} \\ &= -4\sum_{i>j} Re\left(U^*_{\alpha i}U_{\beta i}U_{\alpha j}U^*_{\beta j}\right)\times\sin^2\left(\frac{L\Delta m^2_{ij}}{4E}\right). \end{aligned} \tag{18.40}$$

Similarly, the last term of Eq. (18.38) leads to:

$$\begin{aligned} P_4 &= i\sum_{i\neq j} U^*_{\alpha i}U_{\beta i}U_{\alpha j}U^*_{\beta j}\sin\left(\frac{L\Delta m^2_{ji}}{2E}\right) \\ &= -i\sum_{i>j} 2i\times Im\left(U^*_{\alpha i}U_{\beta i}U_{\alpha j}U^*_{\beta j}\right)\times\sin\left(\frac{L\Delta m^2_{ij}}{2E}\right). \end{aligned}$$

Adding all the probabilities from P_1 to P_4, we may write:

$$\begin{aligned} P(\nu_\alpha \longrightarrow \nu_\beta) &= \delta_{\alpha\beta} - 4\sum_{i>j}\mathrm{Re}\left(U^*_{\alpha i}U_{\beta i}U_{\alpha j}U^*_{\beta j}\right)\times\sin^2\left(\frac{\Delta_{ij}}{2}\right) \\ &\quad +2\sum_{i>j}\mathrm{Im}\left(U^*_{\alpha i}U_{\beta i}U_{\alpha j}U^*_{\beta j}\right)\times\sin\left(\Delta_{ij}\right), \end{aligned} \tag{18.41}$$

$$\text{where}\quad \Delta_{ij} \equiv \frac{\Delta m^2_{ij}}{2E}L = \frac{L}{2E}\left(m^2_i - m^2_j\right). \tag{18.42}$$

For the antineutrino oscillation $\bar{\nu}_\alpha \longrightarrow \bar{\nu}_\beta$, the oscillation probability has the same form as that of Eq. (18.41), except that the last term has a negative sign because for antineutrinos, $U_{\alpha i}$ is replaced by its complex conjugate, which is given as:

$$\begin{aligned} P(\bar{\nu}_\alpha \longrightarrow \bar{\nu}_\beta) = \delta_{\alpha\beta} &- 4\sum_{i>j}\mathrm{Re}\left(U^*_{\alpha i}U_{\beta i}U_{\alpha j}U^*_{\beta j}\right)\times\sin^2\left(\frac{L\Delta m^2_{ij}}{4E}\right) \\ &-2\sum_{i>j}\mathrm{Im}\left(U^*_{\alpha i}U_{\beta i}U_{\alpha j}U^*_{\beta j}\right)\times\sin\left(\frac{L\Delta m^2_{ij}}{2E}\right). \end{aligned} \tag{18.43}$$

https://doi.org/10.1017/9781108489065.019 Published online by Cambridge University Press

For the survival probability, that is, $\alpha = \beta$, we may write the oscillation probability for the neutrinos as:

$$\begin{aligned} P_{\nu_\alpha \to \nu_\alpha}(L,E) &= 1 - 4\sum_{i>j} \mathrm{Re}\big(|U_{\alpha i}|^2 |U_{\alpha j}|^2\big) \sin^2\big(\frac{\Delta m^2_{ij}}{4E} L\big) \\ &\quad + 2\sum_{i>j} \mathrm{Im}\left(|U_{\alpha i}|^2 |U_{\alpha j}|^2\right) \sin\big(\frac{\Delta m^2_{ij}}{2E} L\big). \end{aligned} \tag{18.44}$$

Since $|U_{\alpha i}|^2 |U_{\alpha j}|^2$ is a real quantity, the imaginary part in this equation vanishes, and the general expression for the survival probability is obtained as:

$$P_{\nu_\alpha \to \nu_\alpha}(L,E) = 1 - 4\sum_{i>j} \left(|U_{\alpha i}|^2 |U_{\alpha j}|^2\right) \sin^2\left(\frac{\Delta m^2_{ij}}{4E} L\right). \tag{18.45}$$

For the three flavors of neutrinos $i, j = 1, 2, 3$, as $i > j$, the mass squared difference terms are Δm^2_{32}, Δm^2_{31}, and Δm^2_{21}.

$$\Delta m^2_{32} = m^2_3 - m^2_2 = (m^2_3 - m^2_1) + (m^2_1 - m^2_2) = \Delta m^2_{31} - \Delta m^2_{21} \tag{18.46}$$

and only two of the three Δ_{ij}s, in Eq. (18.41) are independent.

18.2.3 Survival probability for $\nu_\alpha \to \nu_\alpha$

In the disappearance channel, we now express Eq. (18.45) for three-flavor survival probability, as:

$$\begin{aligned} P_{\nu_\alpha \to \nu_\alpha} &= 1 - 4\Big[|U_{\alpha 3}|^2 |U_{\alpha 1}|^2 \sin^2\left(\frac{\Delta_{31}}{2}\right) + |U_{\alpha 3}|^2 |U_{\alpha 2}|^2 \sin^2\left(\frac{\Delta_{32}}{2}\right) \\ &\quad + |U_{\alpha 2}|^2 |U_{\alpha 1}|^2 \sin^2\left(\frac{\Delta_{21}}{2}\right)\Big]. \end{aligned} \tag{18.47}$$

Using Eq. (18.46), we may write:

$$\begin{aligned} P_{\nu_\alpha \to \nu_\alpha} &= 1 - 4\Big[|U_{\alpha 3}|^2 |U_{\alpha 1}|^2 \sin^2\left(\frac{\Delta_{31}}{2}\right) + |U_{\alpha 3}|^2 |U_{\alpha 2}|^2 \sin^2\left(\frac{\Delta_{31}}{2} - \frac{\Delta_{21}}{2}\right) \\ &+ |U_{\alpha 2}|^2 |U_{\alpha 1}|^2 \sin^2\left(\frac{\Delta_{21}}{2}\right)\Big]. \end{aligned} \tag{18.48}$$

Now using the trigonometric identity

$$\sin^2(A - B) = \sin^2 A + \sin^2 B - 2\sin^2 A \sin^2 B - \frac{1}{2}\sin 2A \sin 2B, \tag{18.49}$$

https://doi.org/10.1017/9781108489065.019 Published online by Cambridge University Press

in the third term of Eq. (18.48), that is, $\sin^2\left(\frac{\Delta_{31}}{2}-\frac{\Delta_{21}}{2}\right)$, we may write,

$$\begin{aligned} P_{\nu_\alpha\to\nu_\alpha} &= 1-4\Big[|U_{\alpha3}|^2|U_{\alpha1}|^2\sin^2\left(\frac{\Delta_{31}}{2}\right)+|U_{\alpha3}|^2|U_{\alpha2}|^2\sin^2\left(\frac{\Delta_{31}}{2}\right) \\ &+ |U_{\alpha3}|^2|U_{\alpha2}|^2\sin^2\left(\frac{\Delta_{21}}{2}\right)+|U_{\alpha2}|^2|U_{\alpha1}|^2\sin^2\left(\frac{\Delta_{21}}{2}\right)\Big] \\ &+ 2|U_{\alpha3}|^2|U_{\alpha2}|^2\Big[4\sin^2\left(\frac{\Delta_{31}}{2}\right)\sin^2\left(\frac{\Delta_{21}}{2}\right)+\sin\Delta_{31}\sin\Delta_{21}\Big]. \end{aligned} \tag{18.50}$$

The unitarity condition leads to

$$|U_{\alpha1}|^2+|U_{\alpha2}|^2+|U_{\alpha3}|^2=1$$

and the expression of survival probability is written as:

$$\begin{aligned} P_{\nu_\alpha\to\nu_\alpha} &= 1-4|U_{\alpha3}|^2\Big(1-|U_{\alpha3}|^2\Big)\sin^2\left(\tfrac{\Delta_{31}}{2}\right)-4|U_{\alpha2}|^2\Big(1-|U_{\alpha2}|^2\Big)\sin^2\left(\tfrac{\Delta_{21}}{2}\right) \\ &+2|U_{\alpha3}|^2|U_{\alpha2}|^2\Big[4\sin^2\left(\tfrac{\Delta_{31}}{2}\right)\sin^2\left(\tfrac{\Delta_{21}}{2}\right)+\sin\Delta_{31}\sin\Delta_{21}\Big]. \end{aligned} \tag{18.51}$$

18.2.4 Transition probability for $\nu_\alpha \to \nu_\beta$

Now we will obtain the transition probability when ν_α get converted into another flavor ν_β after the neutrino has traveled a distance L with an energy E. We start with the general expression for probability, given in Eq. (18.41), and simplify it for the three flavor case. This expression takes into account the CP violation phase, therefore we will obtain an expression which can conclude about CP violation in the leptonic sector. In the appearance channel, following a similar step as followed for the disappearance channel, we start with Eq. (18.41), and write:

$$\begin{aligned} P_{\nu_\alpha\to\nu_\beta} &= \delta_{\alpha\beta}-4\Big[\mathrm{Re}\left(U^*_{\alpha3}U_{\beta3}U_{\alpha2}U^*_{\beta2}\right)\sin^2\left(\frac{\Delta_{32}}{2}\right)+\mathrm{Re}\left(U^*_{\alpha3}U_{\beta3}U_{\alpha1}U^*_{\beta1}\right) \\ c\quad & \sin^2\left(\frac{\Delta_{31}}{2}\right)+\mathrm{Re}\left(U^*_{\alpha2}U_{\beta2}U_{\alpha1}U^*_{\beta1}\right)\sin^2\left(\frac{\Delta_{21}}{2}\right)\Big]+2\Big[\mathrm{Im}\left(U^*_{\alpha3}U_{\beta3}U_{\alpha2}U^*_{\beta2}\right) \\ & \sin\Delta_{32}+\mathrm{Im}\left(U^*_{\alpha3}U_{\beta3}U_{\alpha1}U^*_{\beta1}\right)\sin\Delta_{31}+\mathrm{Im}\left(U^*_{\alpha2}U_{\beta2}U_{\alpha1}U^*_{\beta1}\right)\sin\Delta_{21}\Big]. \end{aligned} \tag{18.52}$$

Substituting Eq. (18.46) in Eq. (18.52), we obtain:

$$\begin{aligned} P_{\nu_\alpha\to\nu_\beta} &= -4\Big[\mathrm{Re}\left(U^*_{\alpha3}U_{\beta3}U_{\alpha2}U^*_{\beta2}\right)\sin^2\left(\frac{\Delta_{31}}{2}-\frac{\Delta_{21}}{2}\right)+\mathrm{Re}\left(U^*_{\alpha3}U_{\beta3}U_{\alpha1}U^*_{\beta1}\right)\sin^2\left(\frac{\Delta_{31}}{2}\right) \\ &+\mathrm{Re}\left(U^*_{\alpha2}U_{\beta2}U_{\alpha1}U^*_{\beta1}\right)\sin^2\left(\frac{\Delta_{21}}{2}\right)\Big]+2\Big[\mathrm{Im}\left(U^*_{\alpha3}U_{\beta3}U_{\alpha2}U^*_{\beta2}\right)\sin\left(\Delta_{31}-\Delta_{21}\right) \\ &+\mathrm{Im}\left(U^*_{\alpha3}U_{\beta3}U_{\alpha1}U^*_{\beta1}\right)\sin\Delta_{31}+\mathrm{Im}\left(U^*_{\alpha2}U_{\beta2}U_{\alpha1}U^*_{\beta1}\right)\sin\Delta_{21}\Big]. \end{aligned} \tag{18.53}$$

https://doi.org/10.1017/9781108489065.019 Published online by Cambridge University Press

Now using Eq. (18.49), we may write:

$$\begin{aligned} P_{\nu_\alpha\to\nu_\beta} &= -4\Big[\,\mathrm{Re}\left(U^*_{\alpha3}U_{\beta3}U_{\alpha2}U^*_{\beta2}\right)\left(\sin^2\left(\frac{\Delta_{31}}{2}\right)+\sin^2\left(\frac{\Delta_{21}}{2}\right)-2\sin^2\left(\frac{\Delta_{31}}{2}\right)\sin^2\left(\frac{\Delta_{21}}{2}\right)\right.\\ &\quad\left.-\frac{1}{2}\sin\Delta_{31}\sin\Delta_{21}\right)+Re\left(U^*_{\alpha3}U_{\beta3}U_{\alpha1}U^*_{\beta1}\right)\sin^2\left(\frac{\Delta_{31}}{2}\right)+\mathrm{Re}\left(U^*_{\alpha2}U_{\beta2}U_{\alpha1}U^*_{\beta1}\right)\\ &\quad\sin^2\left(\frac{\Delta_{21}}{2}\right)\Big]+2\Big[\,\mathrm{Im}\left(U^*_{\alpha3}U_{\beta3}U_{\alpha2}U^*_{\beta2}\right)\left(\sin\Delta_{31}\cos\Delta_{21}-\cos\Delta_{31}\sin\Delta_{21}\right)\\ &\quad+\mathrm{Im}\left(U^*_{\alpha3}U_{\beta3}U_{\alpha1}U^*_{\beta1}\right)\sin\Delta_{31}+\mathrm{Im}\left(U^*_{\alpha2}U_{\beta2}U_{\alpha1}U^*_{\beta1}\right)\sin\Delta_{21}\Big]. \end{aligned} \tag{18.54}$$

Making use of the unitarity relation $U_{\alpha1}U^*_{\beta1}+U_{\alpha2}U^*_{\beta2}+U_{\alpha3}U^*_{\beta3}=0$, Eq. (18.54) may be written as:

$$\begin{aligned} P_{\nu_\alpha\to\nu_\beta} &= 4|U_{\alpha3}|^2|U_{\beta3}|^2\sin^2\left(\frac{\Delta_{31}}{2}\right)+4|U_{\alpha2}|^2|U_{\beta2}|^2\sin^2\left(\frac{\Delta_{21}}{2}\right)\\ &\quad+2\,\mathrm{Re}\left(U^*_{\alpha3}U_{\beta3}U_{\alpha2}U^*_{\beta2}\right)\left[4\sin^2\left(\frac{\Delta_{31}}{2}\right)\sin^2\left(\frac{\Delta_{21}}{2}\right)+\sin\Delta_{21}\sin\Delta_{31}\right]\\ &\quad+2\Big[\,\mathrm{Im}\left(U^*_{\alpha3}U_{\beta3}U_{\alpha2}U^*_{\beta2}\right)\sin\Delta_{31}\cos\Delta_{21}-\mathrm{Im}\left(U^*_{\alpha3}U_{\beta3}U_{\alpha2}U^*_{\beta2}\right)\cos\Delta_{31}\sin\Delta_{21}\\ &\quad+\mathrm{Im}\left(U^*_{\alpha3}U_{\beta3}U_{\alpha1}U^*_{\beta1}\right)\sin\Delta_{31}+\mathrm{Im}\left(U^*_{\alpha2}U_{\beta2}U_{\alpha1}U^*_{\beta1}\right)\sin\Delta_{21}\Big]. \end{aligned} \tag{18.55}$$

18.2.5 CP violation in the leptonic sector

The expression of the neutrino transition probability given in Eq. (18.41) may be rewritten as:

$$P_{\nu_\alpha\to\nu_\beta}(L,E) = \delta_{\alpha\beta}+R_{\alpha\beta}+\frac{1}{2}A_{\alpha\beta}, \text{where} \tag{18.56}$$

$$R_{\alpha\beta} = -2\sum_{i>j}\mathrm{Re}\left(U^\star_{\alpha i}U_{\alpha j}U_{\beta i}U^\star_{\beta j}\right)\left(1-\cos\left(\frac{\Delta m^2_{ij}}{2E}L\right)\right), \tag{18.57}$$

$$A_{\alpha\beta} = 4\sum_{i>j}\mathrm{Im}\left(U^\star_{\alpha i}U_{\alpha j}U_{\beta i}U^\star_{\beta j}\right)\sin\left(\frac{\Delta m^2_{ij}}{2E}L\right) \tag{18.58}$$

$$\text{and}\quad P_{\bar\nu_\alpha\to\bar\nu_\beta}(L,E) = \delta_{\alpha\beta}+R_{\alpha\beta}-\frac{1}{2}A_{\alpha\beta}. \tag{18.59}$$

Using these two expressions, we may write:

$$R_{\alpha\beta} = \frac{1}{2}\left(P_{\nu_\alpha\to\nu_\beta}+P_{\bar\nu_\alpha\to\bar\nu_\beta}\right)-\delta_{\alpha\beta}\ \text{and} \tag{18.60}$$

$$A_{\alpha\beta} = P_{\nu_\alpha\to\nu_\beta}-P_{\bar\nu_\alpha\to\bar\nu_\beta}, \tag{18.61}$$

$R_{\alpha\beta}$ and $A_{\alpha\beta}$ are respectively associated with the CP even and CP odd parts of the transition probabilities. $A_{\alpha\beta}$ is a measure of CP violation and will hereafter be written as $A^{\mathrm{CP}}_{\alpha\beta}$. Assuming CPT invariance leads to $A^{\mathrm{CP}}_{\alpha\beta}=-A^{\mathrm{CP}}_{\beta\alpha}$, implying $A^{\mathrm{CP}}_{\alpha\alpha}=0$. If the CP invariance also holds

https://doi.org/10.1017/9781108489065.019 Published online by Cambridge University Press

good, then $A^{\rm CP}_{\alpha\beta} = 0$ for $\alpha \neq \beta$, and therefore it may be concluded that $A^{\rm CP}_{\alpha\beta}$ is a measure of CP asymmetry. A non-zero value of $A^{\rm CP}_{\alpha\beta}$ implies CP violation in the leptonic sector. For a three-flavor neutrino oscillation scenario, $A^{\rm CP}_{e\mu}$, $A^{\rm CP}_{\tau e}$, and $A^{\rm CP}_{\mu\tau}$ are explicitly defined. Following a cyclic permutation among the three flavors of neutrinos, for example, $A^{\rm CP}_{e\mu} = -A^{\rm CP}_{\mu e}$, $A^{\rm CP}_{\tau e} = -A^{\rm CP}_{\tau\mu}$ leads to

$$\begin{aligned} \sum_{\alpha=e,\mu,\tau} A^{\rm CP}_{\alpha\beta} &= 0, \text{ as} \\ \sum_{\alpha=e,\mu,\tau} P_{\nu_\alpha\to\nu_\beta} &= 1 \text{ and } \sum_{\alpha=e,\mu,\tau} P_{\bar{\nu}_\alpha\to\bar{\nu}_\beta} = 1. \end{aligned} \tag{18.62}$$

This relation also gives

$$\sum_{\alpha=\mu,\tau} A^{\rm CP}_{\alpha e} = 0, \sum_{\alpha=e,\tau} A^{\rm CP}_{\alpha\mu} = 0 \quad \text{and} \sum_{\alpha=e,\mu} A^{\rm CP}_{\alpha\tau} = 0. \tag{18.63}$$

We now introduce the Jarlskog invariant $J_{\alpha\beta}$ [1014] defined as:

$$J^{ij}_{\alpha\beta} = \text{Im}\Big(U_{\alpha i} U^*_{\alpha j} U^*_{\beta i} U_{\beta j}\Big), \tag{18.64}$$

such that

$$J^{ij}_{\alpha\beta} = -J^{ji}_{\alpha\beta} \text{ and } J^{ij}_{\beta\alpha} = -J^{ij}_{\alpha\beta}, \;\; i,j = 1,2,3. \tag{18.65}$$

Thus, we may write

$$J_{(\mu,e)} = -J_{(e,\mu)} = J_{(e,\tau)} = -J_{(\tau,e)} = J_{(\tau,\mu)} = -J_{(\mu,\tau)} = \hat{J}\sin\delta \tag{18.66}$$

$$\text{with} \quad \hat{J} = s_{12}c_{12}s_{13}c^2_{13}s_{23}c_{23} = \sin\theta_{12}\cos\theta_{12}\sin\theta_{13}\cos^2\theta_{13}\sin\theta_{23}\cos\theta_{23}. \tag{18.67}$$

Therefore, the value of $J_{\alpha\beta}$ is the same for all flavors. Here,

$$J_{\alpha\beta} \;\; = \;\; \text{Im}(U^*_{\alpha3}U_{\beta3}U_{\alpha1}U^*_{\beta1}) = -\text{Im}(U^*_{\alpha3}U_{\beta3}U_{\alpha2}U^*_{\beta2}) = -\text{Im}(U^*_{\alpha2}U_{\beta2}U_{\alpha1}U^*_{\beta1}).$$

Using Eqs.(18.58) and (18.65), we may write:

$$A^{\rm CP}_{\alpha\beta} = 4J^{21}_{\alpha\beta}\Big(\sin\frac{\Delta m^2_{21}}{2E}L + \sin\frac{\Delta m^2_{32}}{2E}L - \sin\frac{\Delta m^2_{31}}{2E}L\Big). \tag{18.68}$$

Using the relations $\Delta^2_{31} = \Delta^2_{21} + \Delta^2_{32}$ and $\sin\phi + \sin\psi - \sin(\phi+\psi) = 4\sin\frac{\phi}{2}\sin\frac{\psi}{2}\sin\frac{\phi+\psi}{2}$, we may write:

$$A^{\rm CP}_{e\mu} = 16\hat{J}\sin\delta\Big(\sin\frac{\Delta m^2_{12}}{4E}L\;\sin\frac{\Delta m^2_{23}}{4E}L\;\sin\frac{\Delta m^2_{12}+\Delta m^2_{23}}{4E}L\Big). \tag{18.69}$$

https://doi.org/10.1017/9781108489065.019 Published online by Cambridge University Press

In terms of the Jarlskog invariant, the transition probability, Eq. (18.55), may be written as:

$$\begin{aligned} P_{\nu_\alpha \to \nu_\beta} = 4|U_{\alpha 3}|^2|U_{\beta 3}|^2 \sin^2\left(\frac{\Delta_{31}}{2}\right) + 4|U_{\alpha 2}{}^2|U_{\beta 2}{}^2 \sin^2\left(\frac{\Delta_{21}}{2}\right) + 2\,\mathrm{Re}\left(U^*_{\alpha 3}U_{\beta 3}U_{\alpha 2}U^*_{\beta 2}\right) \\ \times\left[4\sin^2\left(\frac{\Delta_{31}}{2}\right)\sin^2\left(\frac{\Delta_{21}}{2}\right) + \sin\Delta_{21}\sin\Delta_{31}\right] - 2J_{\alpha\beta}\sin\Delta_{31}\cos\Delta_{21} \\ +2J_{\alpha\beta}\sin\Delta_{21}\cos\Delta_{31} + 2J_{\alpha\beta}\sin\Delta_{31} - 2J_{\alpha\beta}\sin\Delta_{21} \end{aligned} \tag{18.70}$$

which simplifies to

$$\begin{aligned} P_{\nu_\alpha \to \nu_\beta} \;=\; & 4|U_{\alpha 3}|^2|U_{\beta 3}|^2 \sin^2\left(\frac{\Delta_{31}}{2}\right) + 4|U_{\alpha 2}|^2|U_{\beta 2}|^2 \sin^2\left(\frac{\Delta_{21}}{2}\right) \\ & +2\,\mathrm{Re}\left(U^*_{\alpha 3}U_{\beta 3}U_{\alpha 2}U^*_{\beta 2}\right)\left[4\sin^2\left(\frac{\Delta_{31}}{2}\right)\sin^2\left(\frac{\Delta_{21}}{2}\right) + \sin\Delta_{21}\sin\Delta_{31}\right] \\ & +4J_{\alpha\beta}\left[\sin\Delta_{31}\sin^2\left(\frac{\Delta_{21}}{2}\right) - \sin\Delta_{21}\sin^2\left(\frac{\Delta_{31}}{2}\right)\right]. \end{aligned} \tag{18.71}$$

It may be recalled that the oscillation probability for antineutrinos are obtained by replacing $U_{\alpha i}$ in Eq. (18.32) by its complex conjugate $U^*_{\alpha j}$, which is equivalent to flipping the sign of δ in Eq. (18.35). If CPT invariance is assumed to be an exact conservation law, then

$$P_{\nu_\alpha \to \nu_\beta} = P_{\bar{\nu}_\beta \to \bar{\nu}_\alpha} \quad \text{and} \quad P_{\bar{\nu}_\alpha \to \bar{\nu}_\beta} = P_{\nu_\beta \to \nu_\alpha}.$$

Equivalently, the survival probability as well as the transition probability for antineutrinos may be obtained from Eqs.(18.51) and (18.55) respectively by changing the sign in the Jarlskog invariant term (Eq. (18.71)).

Conditions for non-zero CP violation

- The probability expression given in Eq. (18.71) alongwith $J_{\alpha\beta}$ provides information about the CP violation phase δ_{CP}. It has two parts, one is real and the other is imaginary. The real part has no δ_{CP} term and is known as the CP conserving part. The imaginary part is written in terms of the Jarlskog invariant and its magnitude remains the same for each channel, that is, either we start with ν_μ and end up with ν_e or start with a ν_e and end up with ν_μ and so on.
- The Jarlskog invariant changes sign, that is, for channel $\nu_\mu \to \nu_e$, it is positive; for $\nu_e \to \nu_\mu$, it is negative.
- If any one of the mixing angles is 0 or $\frac{\pi}{2}$, then there is no CP violation in the neutrino sector (as seen from Eq. (18.67)).
- To observe CP violation, we must look for the appearance of a new flavor, that is, we have to measure the probability $P(\nu_\alpha \to \nu_\beta)$ because the probability $P(\nu_\alpha \to \nu_\alpha)$ is always CP conserving.
- To have CP violation, the phase δ_{CP} cannot be 0 or π.
- For the CP violation, all the mass eigenstates should be non-degenerate. If any of the frequencies, say, Δ_{31} or Δ_{21} is zero, the imaginary part of Eq. (18.71) vanishes.

https://doi.org/10.1017/9781108489065.019 Published online by Cambridge University Press

To measure δ_{CP}, we should be able to experimentally measure $(P_{\nu_\alpha\to\nu_\beta} - P_{\bar{\nu}_\alpha\to\bar{\nu}_\beta})$, that is,

$$(P_{\nu_\alpha\to\nu_\beta} - P_{\bar{\nu}_\alpha\to\bar{\nu}_\beta}) = 8\hat{J}\sin\delta\Big[\sin\Delta_{31}\sin^2\left(\frac{\Delta_{21}}{2}\right) - \sin\Delta_{21}\sin^2\left(\frac{\Delta_{31}}{2}\right)\Big]. \quad (18.72)$$

Notice that except for $\sin\delta$, all the other terms are constant for a particular L and E in this expression. Therefore, we may write

$$(P_{\nu_\alpha\to\nu_\beta} - P_{\bar{\nu}_\alpha\to\bar{\nu}_\beta}) \quad = \quad C\sin\delta, \quad (18.73)$$

where

$$C = 8\hat{J}\Big[\sin\Delta_{31}\sin^2\left(\frac{\Delta_{21}}{2}\right) - \sin\Delta_{21}\sin^2\left(\frac{\Delta_{31}}{2}\right)\Big].$$

Measuring $(P_{\nu_\alpha\to\nu_\beta} - P_{\bar{\nu}_\alpha\to\bar{\nu}_\beta})$, δ_{CP} may be calculated.

The T2K and NOvA accelerator experiments have $L = 295$ km and $L = 810$ km baseline, operating at an average neutrino energy $E_\nu = 0.6$ GeV and $E_\nu = 2.0$ GeV, respectively. Both observe transition probability for the channel $\nu_\mu \to \nu_e$ and $\bar{\nu}_\mu \to \bar{\nu}_e$. They study the difference of these probabilities, that is, $A_{\alpha\beta}$, given by Eq. (18.61). From the data of T2K [1000], the best fit value for δ_{CP} has been obtained as -1.87 (-1.43) radian for normal (inverted) ordering, which is a measure of CP violation and it excludes CP conserving values 0 and π at 2σ level.

18.2.6 Series expansions for neutrino oscillation probabilities

In this section, we present the series expansion formulas for three-flavor neutrino oscillation probabilities in vacuum up to second order in α and s_{13}, where $\alpha \equiv \Delta m^2_{21}/\Delta m^2_{31}$ is the mass hierarchy parameter and $s_{13} \equiv \sin\theta_{13}$ is the mixing parameter. We consider the $\nu_\mu \to \nu_e$ channel for the series expansion.

From Eq. (18.55), considering $\alpha = \mu$ and $\beta = e$, and using Eq. (18.66) and Eq. (18.67), we may write

$$\begin{aligned} P(\nu_\mu \to \nu_e) \quad = \quad & 4|U_{\mu3}|^2|U_{e3}|^2\sin^2\left(\frac{\Delta_{31}}{2}\right) + 4|U_{\mu2}|^2|U_{e2}|^2\sin^2\left(\frac{\Delta_{21}}{2}\right) \\ & +2\,\mathrm{Re}\left(U^*_{\mu3}U_{e3}U_{\mu2}U^*_{e2}\right)\Big[4\sin^2\left(\frac{\Delta_{31}}{2}\right)\sin^2\left(\frac{\Delta_{21}}{2}\right) + \sin\Delta_{21}\sin\Delta_{31}\Big] \\ & +4s_{12}c_{12}s_{13}c^2_{13}s_{23}c_{23}\sin\delta_{CP}\Big[\sin\Delta_{31}\sin^2\left(\frac{\Delta_{21}}{2}\right) \\ & -\sin\Delta_{21}\sin^2\left(\frac{\Delta_{31}}{2}\right)\Big]. \end{aligned} \quad (18.74)$$

https://doi.org/10.1017/9781108489065.019 Published online by Cambridge University Press

Using the parameterization of PMNS matrix, we get:

$$\begin{aligned} P(\nu_\mu \to \nu_e) &= 4s_{12}^2c_{13}^2\Big(c_{12}^2c_{23}^2 + s_{12}^2s_{13}^2s_{23}^2 - 2c_{12}c_{23}s_{12}s_{13}s_{23}\cos\delta_{CP}\Big)\sin^2\left(\frac{\Delta_{21}}{2}\right) \\ &\quad +4c_{13}^2s_{23}^2s_{13}^2\sin^2\left(\frac{\Delta_{31}}{2}\right) + 2c_{13}^2s_{23}s_{13}s_{12}\Big(c_{12}c_{23}\cos\delta_{CP} \\ &\quad -s_{12}s_{13}s_{23}\Big)\Big[4\sin^2\left(\frac{\Delta_{31}}{2}\right)\sin^2\left(\frac{\Delta_{21}}{2}\right) + \sin\Delta_{21}\sin\Delta_{31}\Big] \\ &\quad +4s_{12}c_{12}s_{13}c_{13}^2s_{23}c_{23}\sin\delta_{CP} \\ &\quad \Big[\sin\Delta_{31}\sin^2\left(\frac{\Delta_{21}}{2}\right) - \sin\Delta_{21}\sin^2\left(\frac{\Delta_{31}}{2}\right)\Big]. \end{aligned} \tag{18.75}$$

If we take

$$\begin{aligned} \Delta m_{21}^2 &= 7.5\times10^{-5}\text{eV}^2,\ \Delta m_{31}^2 = 2.5\times10^{-3}\text{eV}^2, \\ \alpha &= \frac{\Delta m_{21}^2}{\Delta m_{31}^2} \simeq 0.03, \text{ and } \Delta = \frac{\Delta_{31}}{2}. \end{aligned}$$

For $\theta_{13} = 8.5^\circ$, leading to $s_{13} = \sin\theta_{13} \simeq 0.15$ and $\alpha = 0.03$, which are much smaller than unity, we can expand Eq. (18.75) up to the second order in α and s_{13}, which results in

$$\begin{aligned} P(\nu_\mu \to \nu_e) &= 4s_{12}^2c_{13}^2\Big(c_{12}^2c_{23}^2 + s_{12}^2s_{13}^2s_{23}^2 - 2c_{12}c_{23}s_{12}s_{13}s_{23}\cos\delta_{CP}\Big)\sin^2(\alpha\Delta) \\ &\quad +4c_{13}^2s_{23}^2s_{13}^2\sin^2(\Delta) + 2c_{13}^2s_{23}s_{13}s_{12}\Big(c_{12}c_{23}\cos\delta_{CP} - s_{12}s_{13}s_{23}\Big) \\ &\quad \times\Big[4\sin^2(\Delta)\sin^2(\alpha\Delta) + \sin(2\alpha\Delta)\sin(2\Delta)\Big] \\ &\quad +4s_{12}c_{12}s_{13}c_{13}^2s_{23}c_{23}\sin\delta_{CP}\Big[\sin(2\Delta)\sin^2(\alpha\Delta) - \sin(2\alpha\Delta)\sin^2(\Delta)\Big]. \end{aligned} \tag{18.76}$$

Further, making the approximation $\sin(\alpha\Delta) \simeq \alpha\Delta$ and taking only α and s_{13} up to the second order, we obtain

$$\begin{aligned} P(\nu_\mu \to \nu_e) &\simeq 4s_{12}^2c_{13}^2c_{12}^2c_{23}^2\alpha^2\Delta^2 + 4c_{13}^2s_{23}^2s_{13}^2\sin^2(\Delta) \\ &\quad +4c_{13}^2s_{23}s_{13}s_{12}c_{12}c_{23}\cos(\delta_{CP})\alpha\Delta\sin(2\Delta) \\ &\quad -8s_{12}c_{12}s_{13}c_{13}^2s_{23}c_{23}\sin(\delta_{CP})\alpha\Delta\sin^2(\Delta). \end{aligned} \tag{18.77}$$

For example, taking $\theta_{13} = 8.5^\circ$ leading to $c_{13}^2 \simeq 1$, we obtain:

$$\begin{aligned} P(\nu_\mu \to \nu_e) &= \alpha^2c_{23}^2\sin^2(2\theta_{12})\Delta^2 + 2\alpha s_{13}\sin(2\theta_{23})\sin(2\theta_{12}) \\ &\quad \times\cos(\Delta+\delta_{CP})\Delta\sin(\Delta) + 4s_{23}^2s_{13}^2\sin^2(\Delta). \end{aligned} \tag{18.78}$$

In the T2K kinematic region, we plot a curve for the transition probability $P(\nu_\mu \to \nu_e)$ vs. E, shown in Figure 18.6, for the different values of δ_{CP}, using Eq. (18.78) with $L = 295$ km, $E = 0.05$ GeV to 1 GeV and the global fit value of $\Delta m_{21}^2 = 7.5\times10^{-5}\text{eV}^2$, $\Delta m_{31}^2 = 2.5\times10^{-3}\text{eV}^2$, $\theta_{12} = 34.5^\circ$, $\theta_{23} = 45^\circ$ and $\theta_{13} = 8.5^\circ$.

https://doi.org/10.1017/9781108489065.019 Published online by Cambridge University Press

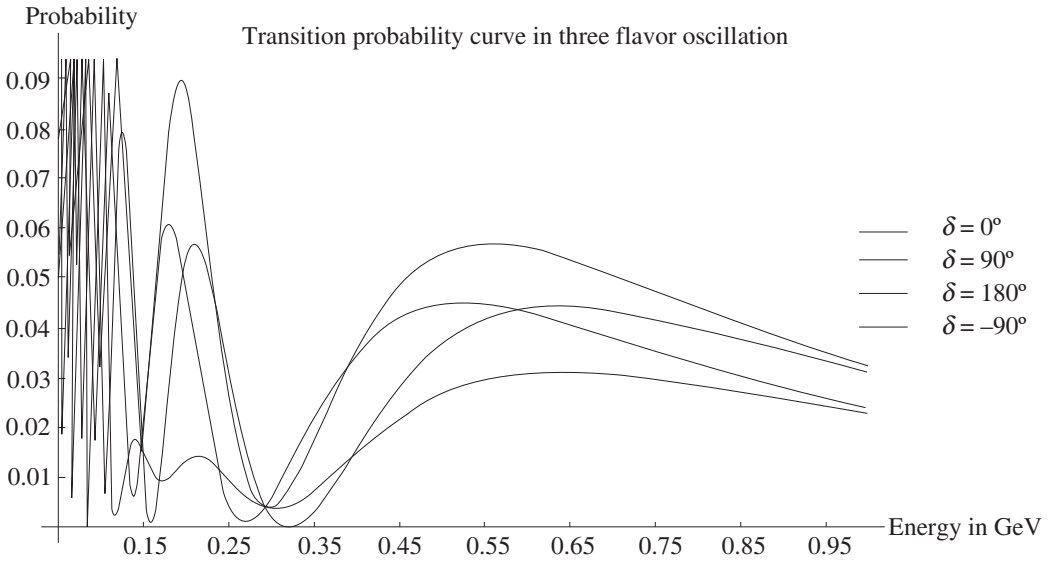

Figure 18.6 Appearance probability curve in three-flavor neutrino oscillations for different values of δ_{cp}.

A similar plot has been shown in Figure 18.7, where the transition probability curve for $P(\bar{\nu_\mu} \rightarrow \bar{\nu_e})$ vs. E has been shown by replacing δ_{CP} with -δ_{CP} in Eq. (18.78). The observation of transition probability in the appearance experiments where both the neutrino and antineutrino channels are simultaneously studied gives information about δ_{CP}.

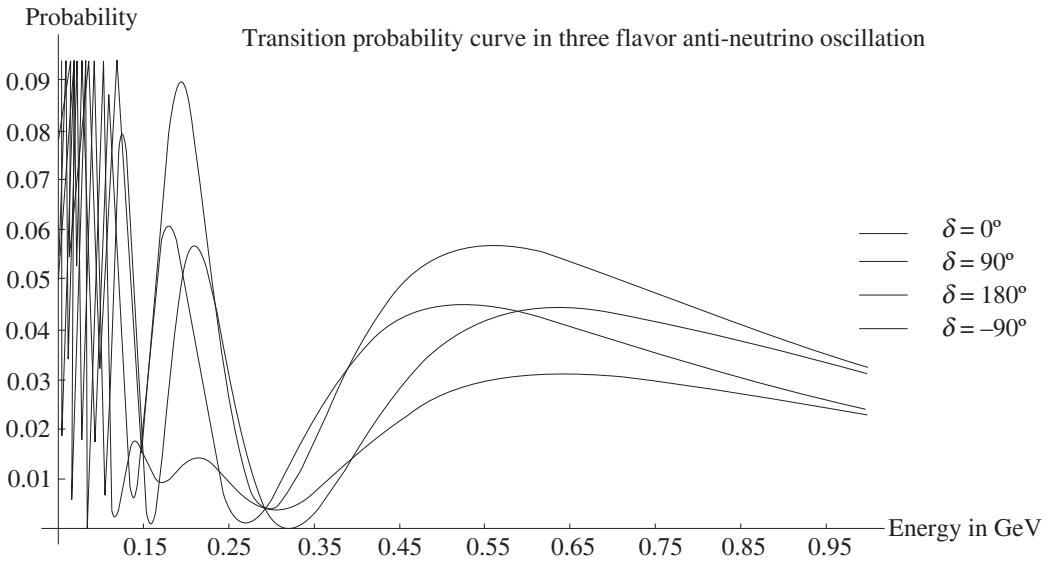

Figure 18.7 Appearance probability curve in three-flavor antineutrino oscillations for different values of δ_{CP}.

https://doi.org/10.1017/9781108489065.019 Published online by Cambridge University Press

18.2.7 Neutrino mass hierarchy: Normal and inverted

When there are three neutrino flavor eigenstates and three mass eigenstates, there are two nonequivalent orderings for the neutrino masses as shown in Figure 18.8. They are called normal ordering (NO) when $m_1 < m_2 < m_3$, and inverted ordering (IO) when $m_3 < m_1 < m_2$. For such cases, two of the neutrino mass eigenstates are nearly degenerate. If these states are chosen to be m_1 and m_2, then,

$$|\Delta m^2_{21}| \equiv \Delta m^2_{\rm small} \quad \text{and} \quad |\Delta m^2_{31}| \cong |\Delta m^2_{32}| \equiv \Delta m^2_{\rm big}\,. \tag{18.79}$$

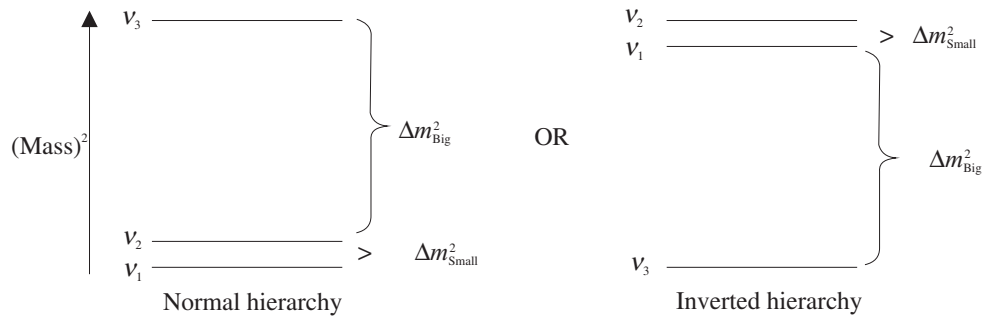

Figure 18.8 A three-neutrino (mass)^2 spectrum in which the $\nu_2 - \nu_1$ splitting $\Delta m^2_{\rm small}$ is much smaller than the splitting $\Delta m^2_{\rm big}$ between ν_3 and the $\nu_2 - \nu_1$ pair. The later pair may be at either the bottom or the top of the spectrum.

The smaller one is always Δm^2_{21}, while the larger one is generally denoted by $\Delta m^2_{3\ell}$, with $\ell = 2$ for normal ordering and $\ell = 1$ for inverted ordering [1015]. Hence,

$$\Delta m^2_{3\ell} = \begin{cases} \Delta m^2_{32} = m^2_3 - m^2_2 > 0 & \text{for NO}\,, \\ \Delta m^2_{31} = m^2_3 - m^2_1 < 0 & \text{for IO}\,. \end{cases} \tag{18.80}$$

From the analysis of neutrino oscillation data, it follows that one mass squared difference is much smaller than the other. Correspondingly, two scenarios for the three-neutrino mass spectra are possible:

1. Normal hierarchy (NH): $\Delta m^2_{21} \ll \Delta m^2_{32}$.
2. Inverted hierarchy (IH): $\Delta m^2_{21} \ll |\Delta m^2_{31}|$.

Let us denote two independent neutrino mass squared differences Δm^2_S (solar) and Δm^2_A (atmospheric). We have

$$\Delta m^2_{21} = \Delta m^2_S,\ \Delta m^2_{32} = \Delta m^2_A \ \ (\text{NH}), \tag{18.81}$$

$$\Delta m^2_{21} = \Delta m^2_S, \text{ and } \Delta m^2_{31} = -\Delta m^2_A \ \ (\text{IH}). \tag{18.82}$$

Let us recall the expression of transition probability given in Eq. (18.37)

$$P(\nu_\alpha \longrightarrow \nu_\beta) = \left| \sum_j U_{\alpha j} e^{2i\Delta_{qj}} U^*_{\beta j} \right|^2, \tag{18.83}$$

https://doi.org/10.1017/9781108489065.019 Published online by Cambridge University Press

where q is an arbitrary fixed index and

$$\Delta_{qj} = \frac{\Delta m^2_{qj} L}{4E}.$$

Using the unitarity of the mixing matrix, we can rewrite this expression as:

$$P(\nu_\alpha \longrightarrow \nu_\beta) = \left| \delta_{\alpha\beta} + \sum_j U_{\alpha j}(e^{2i\Delta_{qj}} - 1)U^*_{\beta j} \right|^2 \tag{18.84}$$

$$= \left| \delta_{\alpha\beta} + 2i \sum_j U_{\alpha j} U^*_{\beta j} e^{i\Delta_{qj}} \sin\Delta_{qj} \right|^2 . \tag{18.85}$$

Finally, we obtain the following general expression for the transition probability for neutrinos $(\nu_\alpha \to \nu_\beta)$ and antineutrinos $(\bar{\nu}_\alpha \to \bar{\nu}_\beta)$:

$$\begin{aligned} P(\nu_\alpha(\bar{\nu}_\alpha) \longrightarrow \nu_\beta(\bar{\nu}_\beta)) \;=\; & \delta_{\alpha\beta} - 4\sum_j |U_{\alpha j}|^2(\delta_{\alpha\beta} - |U_{\beta j}|^2)\sin^2(\Delta_{qj}) \\ & + 8\sum_{j>k} Re(U_{\beta j}U^*_{\alpha j}U^*_{\beta k}U_{\alpha k})\cos(\Delta_{qj} - \Delta_{qk})\sin\Delta_{qj}\sin\Delta_{qk} \\ & \mp 8\sum_{j>k} Im(U_{\beta j}U^*_{\alpha j}U^*_{\beta k}U_{\alpha k})\sin(\Delta_{qj} - \Delta_{qk})\sin\Delta_{qj}\sin\Delta_{qk}. \end{aligned}$$

In the case of the NH, it is natural to choose $q = 2$. From the general expression, we have:

$$\begin{aligned} P^{NH}(\nu_\alpha(\bar{\nu}_\alpha) \longrightarrow \nu_\beta(\bar{\nu}_\beta)) = {} & \delta_{\alpha\beta} - 4|U_{\alpha 1}|^2(\delta_{\alpha\beta} - |U_{\beta 1}|^2)\sin^2\Delta_S - 4|U_{\alpha 3}|^2(\delta_{\alpha\beta} - |U_{\beta 3}|^2) \\ & \sin^2\Delta_A - 8\,\mathrm{Re}\,[U_{\beta 3}U^*_{\alpha 3}U^*_{\beta 1}U_{\alpha 1}]\cos(\Delta_A + \Delta_S)\sin\Delta_A\sin\Delta_S \\ & \mp 8\,\mathrm{Im}\,[U_{\beta 3}U^*_{\alpha 3}U^*_{\beta 1}U_{\alpha 1}]\sin(\Delta_A + \Delta_S)\sin\Delta_A\sin\Delta_S. \end{aligned} \tag{18.86}$$

In the case of the IH, we choose $q = 1$. For the transition probability, we obtain the following expression:

$$\begin{aligned} P^{IH}(\nu_\alpha(\bar{\nu}_\alpha) \longrightarrow \nu_\beta(\bar{\nu}_\beta)) = {} & \delta_{\alpha\beta} - 4|U_{\alpha 2}|^2(\delta_{\alpha\beta} - |U_{\beta 2}|^2)\sin^2\Delta_S - 4|U_{\alpha 3}|^2(\delta_{\alpha\beta} - |U_{\beta 3}|^2) \\ & \sin^2\Delta_A - 8\,\mathrm{Re}\,[U_{\beta 3}U^*_{\alpha 3}U^*_{\beta 2}U_{\alpha 2}]\cos(\Delta_A + \Delta_S)\sin\Delta_A\sin\Delta_S \\ & \pm 8\,Im\,[U_{\beta 3}U^*_{\alpha 3}U^*_{\beta 2}U_{\alpha 2}]\sin(\Delta_A + \Delta_S)\sin\Delta_A\sin\Delta_S. \end{aligned} \tag{18.87}$$

Notice that the expressions given in Eq. (18.86) and Eq. (18.87) differ by the change $U_{\alpha 1} \to U_{\alpha 2}$ and by the sign of the last term. Also notice that for the CP asymmetry from Eq. (18.86) and Eq. (18.87), we may write:

$$A^{CP}_{\alpha\beta} = -16\,\mathrm{Im}\,[U_{\beta 3}U^*_{\alpha 3}U^*_{\beta 1}U_{\alpha 1}]\sin(\Delta_A + \Delta_S)\sin\Delta_A\sin\Delta_S \tag{18.88}$$

in the case of NH and

$$A^{CP}_{\alpha\beta} = 16\,\mathrm{Im}\,[U_{\beta 3}U^*_{\alpha 3}U^*_{\beta 2}U_{\alpha 2}]\sin(\Delta_A + \Delta_S)\sin\Delta_A\sin\Delta_S \tag{18.89}$$

https://doi.org/10.1017/9781108489065.019 Published online by Cambridge University Press

in the case of IH. If we take $\Delta m^2_S = 7.39 \times 10^{-5}\text{eV}^2$ and $\Delta m^2_A = 2.5 \times 10^{-3}\text{eV}^2$, then

$$\frac{\Delta m^2_S}{\Delta m^2_A} \simeq 3 \cdot 10^{-2}, \quad \text{and} \quad \sin^2\theta_{13} \simeq 2.4 \cdot 10^{-2}. \tag{18.90}$$

It may be noticed that the effect of $\frac{L}{E}$ ($\frac{\Delta m^2_A L}{2E} \gtrsim 1$) on the neutrino oscillations are large in the energy region of the atmospheric neutrinos; we can neglect the small contributions from Δm^2_S and $\sin^2\theta_{13}$ in the transition probabilities. We obtain the following expressions for the survival probabilities for $\nu_\mu(\bar{\nu}_\mu)$:

$$\begin{aligned} P^{NH}(\nu_\alpha \to \nu_\alpha) &\simeq P^{IH}(\nu_\alpha \to \nu_\alpha) \simeq 1 - 4|U_{\mu 3}|^2(1 - |U_{\mu 3}|^2)\sin^2\Delta m^2_A \frac{L}{4E} \\ &= 1 - \sin^2 2\theta_{23}\sin^2\Delta m^2_A \frac{L}{4E}. \end{aligned} \tag{18.91}$$

Now, we have $P(\nu_\mu \to \nu_e) \simeq 0$ with this approximation:

$$P(\nu_\mu \to \nu_\tau) \simeq 1 - P(\nu_\mu \to \nu_\mu) \simeq \sin^2 2\theta_{23}\sin^2\Delta m^2_A \frac{L}{4E}. \tag{18.92}$$

Thus, in the energy region of the atmospheric neutrinos, predominantly $\nu_\mu \rightleftarrows \nu_\tau$ oscillations take place.

Let us now consider $\bar{\nu}_e$ oscillation in the energy region of the KamLAND reactor ($\frac{\Delta m^2_S L}{2E} \gtrsim 1$). Neglecting the contribution of $\sin^2\theta_{13}$:

$$P^{NH}(\bar{\nu}_e \to \bar{\nu}_e) \simeq P^{IH}(\bar{\nu}_e \to \bar{\nu}_e) \simeq 1 - \sin^2 2\theta_{12}\sin^2\Delta m^2_S \frac{L}{4E}, \tag{18.93}$$

$$P^{NH}(\bar{\nu}_e \to \bar{\nu}_\mu) \simeq P^{IH}(\bar{\nu}_e \to \bar{\nu}_\mu) \simeq \sin^2 2\theta_{12}\cos^2\theta_{23}\sin^2\Delta m^2_S \frac{L}{4E} \tag{18.94}$$

and

$$P^{NH}(\bar{\nu}_e \to \bar{\nu}_\tau) \simeq P^{IH}(\bar{\nu}_e \to \bar{\nu}_\tau) \simeq \sin^2 2\theta_{12}\sin^2\theta_{23}\sin^2\Delta m^2_S \frac{L}{4E} \tag{18.95}$$

which gives:

$$P(\bar{\nu}_e \to \bar{\nu}_e) = 1 - P(\bar{\nu}_e \to \bar{\nu}_\mu) - P(\bar{\nu}_e \to \bar{\nu}_\tau) \tag{18.96}$$

and

$$\frac{P(\bar{\nu}_e \to \bar{\nu}_\tau)}{P(\bar{\nu}_e \to \bar{\nu}_\mu)} \simeq \tan^2\theta_{23} \simeq 1. \tag{18.97}$$

Using Eq. (18.91) and (18.93), the Super-Kamiokande detector analyzed their atmospheric neutrino samples; K2K and MINOS used them in the analysis of accelerator neutrino experiments and KamLAND used it in the analysis of reactor antineutrino experiments.

https://doi.org/10.1017/9781108489065.019 Published online by Cambridge University Press

18.3 Neutrino Oscillation in Matter

While deriving the probabilities for neutrino oscillation in vacuum in the previous section, we have not considered the fact that neutrinos may also be affected by the matter they traverse, leading to possible modifications of the transition probabilities. There are examples like the solar neutrinos which are produced deep inside the core of the sun and traverse different layers like the core, radiation zone, convection zone, photosphere, chromosphere to corona which have different matter densities (Figure 18.9). Moreover, neutrinos passing through the earth like

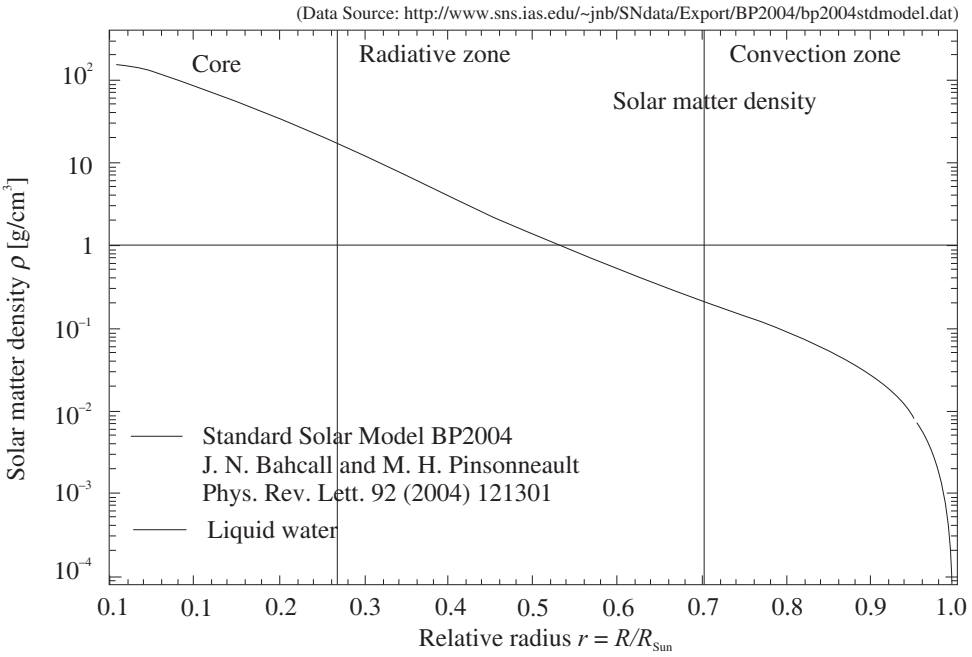

Figure 18.9 Matter density variation inside the sun [1016].

atmospheric neutrinos coming from the other side of the globe traverse the core, mantle, and the crust of earth having different densities, as shown in Figure 18.10, before getting detected. During a solar eclipse, neutrinos from the sun have to pass through the moon and the earth before reaching the detection point. Moreover, neutrinos coming from different sources to the detectors like DUNE, JUNO, KamLAND, MINOS, T2K etc. get affected by the earth matter. In a pioneering work, Wolfenstein [1010] and later Mikheyev and Smirnov [1009] showed that the parameters of neutrino oscillation may be significantly modified if the neutrino travels through matter rather than vacuum. In the next section, we study the neutrino–matter interactions which affects the neutrino properties and modifies the oscillation probabilities when neutrinos travel through the matter.

https://doi.org/10.1017/9781108489065.019 Published online by Cambridge University Press

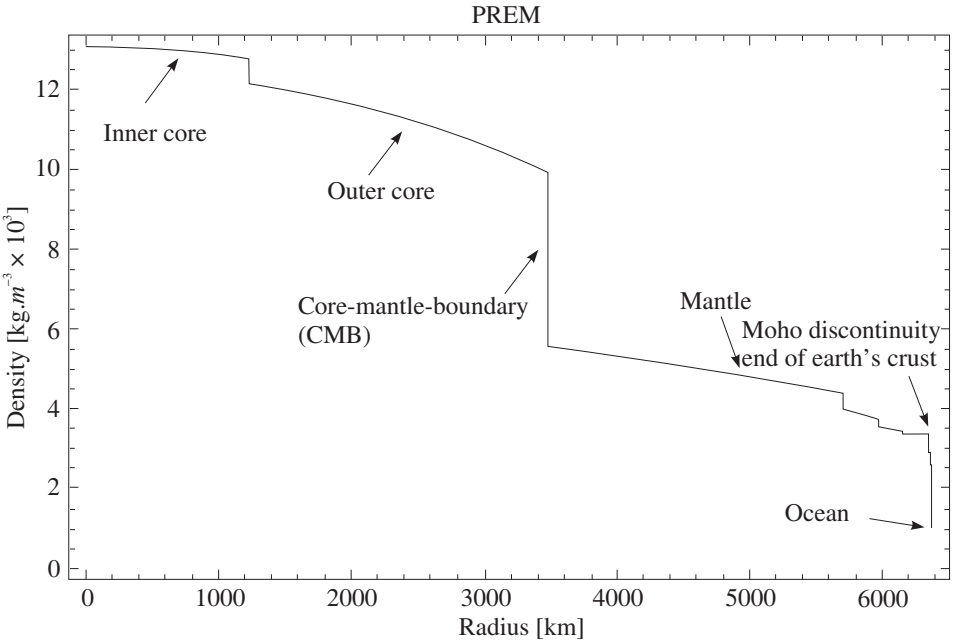

Figure 18.10 Matter density variation inside the earth [1017].

18.3.1 Effective potential for neutrino–matter interactions

When neutrinos propagate through matter, their properties may change because of their interaction with matter. Neutrinos of all flavors interact with matter via charge current (CC) and neutral current (NC) interaction; the nature of their interaction with matter depends upon their energy. For example, neutrinos (ν_e) being produced in the sun have energies less than 20 MeV, and they oscillate into ν_μ or ν_τ ($\nu_e \rightarrow \nu_\mu$) and ($\nu_e \rightarrow \nu_\tau$), through charged current reactions like:

$$\nu_\mu + n \rightarrow \mu^- + p \qquad \text{and} \qquad \nu_\tau + n \rightarrow \tau^- + p$$

are not possible due to the large mass of μ (m_μ=105.658 MeV) and τ (m_τ=1776.84 MeV) leptons; however, neutral current reactions like $\nu_l + n/p \rightarrow \nu_l + n/p, \;\; l = \mu, \tau$ are possible. Therefore, while the original matter which consists of mainly electrons, protons, and neutrons undergo neutral current interactions with all flavors of neutrinos through $\nu_l e \rightarrow \nu_l e, \nu_l p \rightarrow \nu_l p$, $\nu_l n \rightarrow \nu_l n$ ($l = e, \mu, \tau$) processes, they undergo only charged current (CC) interactions with ν_e and $\bar{\nu}_e$, that is, $\nu_e n \rightarrow e^- p$ and $\bar{\nu}_e p \rightarrow e^+ n$

In this section, we calculate the effective potentials derived from the effective CC and NC interaction through coherent neutrino scattering in matter. The Feynman diagrams for the CC and NC reactions are shown in Figure 18.11. First, we estimate the effective potential arising due to CC interactions.

https://doi.org/10.1017/9781108489065.019 Published online by Cambridge University Press

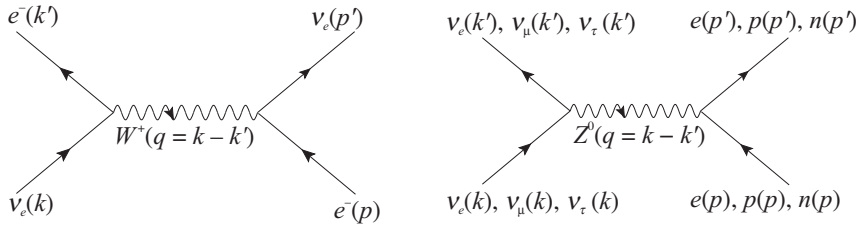

Figure 18.11 (a) Charged current interaction (left). (b) Neutral current interaction (right).

(i) Charged current reactions: Consider the reaction:

$$\nu_e + e^- \rightarrow \nu_e + e^-. \tag{18.98}$$

The Feynman diagram contributing to this reaction is shown in Figure 18.11(a). The interaction Hamiltonian is written as:

$$H_{CC} = \frac{G_F}{\sqrt{2}} \left[\left(\bar{u}_e | \gamma^\mu (1 - \gamma^5) | u_{\nu_e} \right) \left(\bar{u}_{\nu_e} \gamma_\mu (1 - \gamma^5) u_e \right) \right]. \tag{18.99}$$

Using the Fierz transformation, it can be written as:

$$H_{CC} = \frac{G_F}{\sqrt{2}} \left[\left(\bar{u}_e | \gamma^\mu (1 - \gamma^5) | u_e \right) \left(\bar{u}_{\nu_e} \gamma_\mu (1 - \gamma^5) u_{\nu_e} \right) \right], \tag{18.100}$$

where G_F is the Fermi coupling constant and u_{ν_e} and u_e represents the fields of electron type neutrino and electron, respectively.

The aforementioned interaction Hamiltonian is written for free electrons and neutrinos. It occurs when a neutrino moves in the medium of matter with solar, atmospheric, or earth matter environment in which the electrons are essentially nonrelativistic as are protons and neutrons. For example, even in the core of the sun where the temperature is fifteen million degree Celsius, the electron's energy are in the keV region corresponding to $\frac{kT}{m_e} \sim 10^{-3}$. A nonrelativistic reduction of the spinors $u_{e,p,n}$ in Eq. (18.100) can be made before taking the expectation value between the initial and final states of the nonrelativistic electrons, that is, $\vec{p} \rightarrow 0$, making the neutrino momenta to be the same in the initial as well as in the final states. We find that the energy corresponding to the Hamiltonian in Eq. (18.100) is given by:

$$\mathcal{E} = \langle H \rangle = \frac{G_F}{\sqrt{2}} \left[\left\langle \bar{u}_e(\vec{p} = 0) | \gamma^\mu (1 - \gamma^5) | u_e(\vec{p} = 0) \right\rangle \left\langle \bar{u}_\nu(\vec{k}) \gamma_\mu (1 - \gamma_5) u_\nu(\vec{k}) \right\rangle \right]. \tag{18.101}$$

$$\text{Here,} \quad \langle \bar{u}_e \gamma^0 u_e \rangle = \langle {u_e}^\dagger u_e \rangle = N_e, \qquad \langle \bar{u}_e \gamma^i u_e \rangle = \langle \frac{\vec{p}}{m_e} \rangle \simeq 0,$$

$$\langle \bar{u}_e \gamma^0 \gamma^5 u_e \rangle \simeq \langle \frac{\vec{\sigma} \cdot \vec{p}}{m_e} \rangle \simeq 0, \qquad \langle \bar{u}_e \gamma^i \gamma^5 u_e \rangle \simeq \langle \vec{\sigma} \rangle,$$

where N_e is the number density of the electrons and $\langle \vec{\sigma} \rangle$ is the average spin of the electrons. Since the matter in the sun or in the atmosphere is normalized in the spin space, that is, $\langle \vec{\sigma} \rangle \simeq 0$, the energy density corresponding to the Hamiltonian is written as

https://doi.org/10.1017/9781108489065.019 Published online by Cambridge University Press

$$H_{CC} = \frac{G_F}{\sqrt{2}} N_e . \langle \bar{u}_{\nu_e} \gamma_0 (1-\gamma^5) u_{\nu_e} \rangle = \sqrt{2} G_F N_e (u^\dagger_{\nu_e} u_{\nu_e}) = \sqrt{2} G_F N_e. \tag{18.102}$$

(ii) Neutral current reactions: Consider the reaction:

$$\nu_\alpha + X_\beta \rightarrow \nu_\alpha + X_\beta,$$

where $\alpha = e, \mu, \tau$ and $X_\beta = e, p, n$. The Feynman diagram corresponding to this equation is shown in Figure 18.11(b). All the neutrino flavors contribute equally to the effective potential in this case. The effective potential is obtained by including the electron, proton, and neutron background such that the interaction Hamiltonian for the NC is given by:

$$\begin{aligned} H_{NC} = \frac{G_F}{\sqrt{2}} \Bigg[& \langle \bar{u}_e \gamma^\mu (g^e_V - g^e_A \gamma^5) u_e \rangle \sum_\alpha \bar{u}_{\nu_\alpha} \gamma^\mu (g^\nu_V - g^\nu_A \gamma^5) u_{\nu_\alpha} \\ & + \langle \bar{u}_p \gamma^\mu (g^p_V - g^p_A \gamma^5) u_p \rangle \sum_\alpha \bar{u}_{\nu_\alpha} \gamma^\mu (g^\nu_V - g^\nu_A \gamma^5) u_{\nu_\alpha} \\ & + \langle \bar{u}_n \gamma^\mu (g^n_V - g^n_A \gamma^5) u_n \rangle \sum_\alpha \bar{u}_{\nu_\alpha} \gamma^\mu (g^\nu_V - g^\nu_A \gamma^5) u_{\nu_\alpha} \Bigg], \end{aligned} \tag{18.103}$$

where

$$g^p_V = \frac{1}{2} - 2\sin^2\theta_w = -g^e_V, \qquad g^p_A = \frac{1}{2} = -g^e_A,$$

$$g^n_V = g^n_A = -\frac{1}{2}, \quad \text{and for neutrinos } g^\nu_V = 1 \text{ and } g^\nu_A = 1.$$

Since, in matter, the number of electrons are equal to the number of protons, and g_A and g_V for electrons and protons are equal in magnitude and opposite in sign, their contributions cancel out and we are left only with the contribution from the neutron

$$\begin{aligned} H^n_{NC} &= \frac{G_F}{\sqrt{2}} \left[\langle \bar{u}_n \gamma^0 (-\frac{1}{2} + \frac{1}{2}\gamma^5) u_n \rangle \sum_\alpha \bar{u}_{\nu_\alpha} \gamma^0 (1-\gamma^5) u_{\nu_\alpha} \right] \\ &\simeq -\frac{G_F}{\sqrt{2}} N_n \sum_\alpha \bar{u}_{\nu_\alpha} \gamma^0 u_{\nu_\alpha}, \\ \Rightarrow \quad V^n_{NC} &= G_F \left(-\frac{N_n}{\sqrt{2}} \right). \end{aligned} \tag{18.104}$$

The effective potential due to CC and NC reactions is

$$V = V^e_{CC} + V^n_{NC} = \sqrt{2} G_F (N_e \delta_{\alpha e} - \frac{1}{2} N_n). \tag{18.105}$$

We have derived the expressions for V_{CC} and V_{NC} for neutrinos; for antineutrinos, their signs will get reversed, that is,

$$V_{CC}(\bar{\nu}_e) = -\sqrt{2} G_F N_e, \qquad V_{NC}(\bar{\nu}_\alpha) = -G_F \left(-\frac{N_n}{\sqrt{2}} \right). \tag{18.106}$$

https://doi.org/10.1017/9781108489065.019 Published online by Cambridge University Press

The value of V_{CC} is given by:

$$V_{CC} \simeq 7.6 \times 10^{-14} \Big(\frac{\rho}{\mathrm{g/cm^3}}\Big) Y_e \quad \mathrm{eV}, \tag{18.107}$$

where $Y_e \sim 0.5$. The strength of V_{CC} inside the sun, the earth, and supernova is given in Table 18.1. Due to this extra potential V_{CC}, the effective mass of an electron in the matter gets modified. Using the relativistic energy–momentum relation,

$$m^2_{e(\mathrm{matter})} = (E + V_{CC})^2 - |\vec{p}|^2 = E^2 - |\vec{p}|^2 + V^2_{CC} + 2V_{CC}E.$$

Table 18.1 The impact of matter potential in various medium.

Medium	Matter density$(\mathrm{g/cm^3})$	V_{CC}(eV)
Solar core	~ 100	$\sim 10^{-12}$
Earth core	~ 10	$\sim 10^{-13}$
Supernova	$\sim 10^{14}$	~ 1

Since $E >> V_{CC}$, V^2_{CC} is neglected; then,

$$m^2_{e(\mathrm{matter})} = m^2_e + 2V_{CC}E \qquad \Rightarrow \Delta m^2 = 2EV_{CC},$$

where $\Delta m^2 = m^2_{e(\mathrm{matter})} - m^2_e$. Using V_{CC} from Eq. (18.106), we may write:

$$\Delta m^2 = 2\sqrt{2}EG_F N_e. \tag{18.108}$$

18.3.2 Interaction Hamiltonian in matter

Let us now consider the evolution of two neutrino flavors in ordinary matter. First, we consider the case where the density of matter ρ is constant. For this, we work out the Hamiltonian for neutrinos traveling in vacuum and then we will see how it gets modified in the case of matter.

For medium with constant density, let us consider the time-dependent Schrödinger equation in the Lab frame for a neutrino traveling through vacuum ($c = \hbar = 1$), that is,

$$i\frac{\partial}{\partial t}|\nu(t)\rangle = H|\nu(t)\rangle, \tag{18.109}$$

where for two neutrino flavors e and μ

$$|\nu(t)\rangle = \begin{pmatrix} \nu_e(t) \\ \nu_\mu(t) \end{pmatrix}, \tag{18.110}$$

https://doi.org/10.1017/9781108489065.019 Published online by Cambridge University Press

where $\nu_\alpha(t)(\alpha = e, \mu)$ is the amplitude for ν being a ν_α at time t. Now writing the Hamiltonian for neutrino oscillation in vacuum

$$\begin{aligned}\langle\nu_\alpha|H_{\text{vacuum}}|\nu_\beta\rangle &= \langle\sum_i U_{\alpha i}\nu_i|H_{\text{vacuum}}|\sum_j U_{\beta j}\nu_j\rangle \\ &= \sum_i U^*_{\alpha i}\langle\nu_i|H_{\text{vacuum}}|\nu_i\rangle U_{\beta i} = \sum_i U^*_{\alpha i}E_i U_{\beta i}, \end{aligned} \tag{18.111}$$

where U is the same as used in Eq. (18.9) and U^* is the complex conjugate of U, such that

$$\begin{aligned}\Rightarrow\ \langle\nu_\alpha|H_{\text{vacuum}}|\nu_\beta\rangle &= \begin{pmatrix}\cos\theta & -\sin\theta\\ \sin\theta & \cos\theta\end{pmatrix}\begin{pmatrix}E_1 & 0\\ 0 & E_2\end{pmatrix}\begin{pmatrix}\cos\theta & \sin\theta\\ -\sin\theta & \cos\theta\end{pmatrix} \\ &= \begin{pmatrix}E_1\cos^2\theta + E_2\sin^2\theta & E_1\sin\theta\cos\theta - E_2\sin\theta\cos\theta\\ E_1\sin\theta\cos\theta - E_2\sin\theta\cos\theta & E_1\sin^2\theta + E_2\cos^2\theta\end{pmatrix} \\ &= \begin{pmatrix}H_{\alpha\alpha} & H_{\alpha\beta}\\ H_{\beta\alpha} & H_{\beta\beta}\end{pmatrix}. \end{aligned} \tag{18.112}$$

In this expression, E_1 and E_2 are ultra-relativistic energies of the neutrino mass eigenstates. In Eq. (18.112), let us first solve $H_{\alpha\alpha}$:

$$\begin{aligned}H_{\alpha\alpha} &= E_1\cos^2\theta + E_2\sin^2\theta = \sqrt{|\vec{p}|^2 + m_1^2}\cos^2\theta + \sqrt{|\vec{p}|^2 + m_2^2}\sin^2\theta \\ &= -\cos(2\theta)\,\frac{\Delta m^2}{4|\vec{p}|} + |\vec{p}| + \frac{m_1^2 + m_2^2}{4|\vec{p}|},\ \text{where } \Delta m^2 = m_2^2 - m_1^2.\end{aligned}$$

Similarly, we may write:

$$\begin{aligned}H_{\beta\beta} &= \cos(2\theta)\,\frac{\Delta m^2}{4|\vec{p}|} + |\vec{p}| + \frac{m_1^2 + m_2^2}{4|\vec{p}|} \\ \text{and}\quad H_{\alpha\beta} &= H_{\beta\alpha} = \sin(2\theta)\frac{\Delta m^2}{4|\vec{p}|}.\end{aligned}$$

Therefore, collecting all the terms appearing in Eq. (18.112), we get:

$$H_{\text{vacuum}} = \frac{\Delta m^2}{4|\vec{p}|}\begin{pmatrix}-\cos(2\theta) & \sin(2\theta)\\ \sin(2\theta) & \cos(2\theta)\end{pmatrix} + \left(|\vec{p}| + \frac{m_1^2 + m_2^2}{4|\vec{p}|}\right)\begin{pmatrix}1 & 0\\ 0 & 1\end{pmatrix}.$$

We will concentrate only on the first term of H_{vacuum} as the relative phases of the interfering terms is important and consequently, the relative energies are important. Therefore, the Hamiltonian for the highly relativistic neutrinos may be approximated as:

$$H_{\text{vacuum}} \simeq \frac{\Delta m^2}{4E}\begin{pmatrix}-\cos(2\theta) & \sin(2\theta)\\ \sin(2\theta) & \cos(2\theta)\end{pmatrix}.$$

The equation of motion becomes

$$i\begin{bmatrix}\dot{\nu}_e(t)\\ \dot{\nu}_\mu(t)\end{bmatrix} = H_{\text{vacuum}}\begin{bmatrix}\nu_e(t)\\ \nu_\mu(t)\end{bmatrix} = \frac{\Delta m^2}{4E}\begin{pmatrix}-\cos(2\theta) & \sin(2\theta)\\ \sin(2\theta) & \cos(2\theta)\end{pmatrix}\begin{bmatrix}\nu_e(t)\\ \nu_\mu(t)\end{bmatrix}. \tag{18.113}$$

https://doi.org/10.1017/9781108489065.019 Published online by Cambridge University Press

In matter, the modified Hamiltonian may be written as:

$$H_M = H_{\text{vacuum}} + V_{CC}^e \begin{pmatrix} 1 & 0 \\ 0 & 0 \end{pmatrix} + V_{NC}^n \begin{pmatrix} 1 & 0 \\ 0 & 1 \end{pmatrix}.$$

Here, V_{CC} is the extra potential faced by the electron type neutrino during its charged-current interaction and V_{NC} is the extra potential arising due to the NC interaction of all flavors of neutrino. The V_{NC} term includes contributions from both diagonal elements, so we use an identity matrix. We can re-write the aforementioned expression as:

$$H_M = H_{\text{vacuum}} + \frac{1}{2} V_{CC} \begin{pmatrix} 1 & 0 \\ 0 & -1 \end{pmatrix} + \frac{1}{2} V_{CC} \begin{pmatrix} 1 & 0 \\ 0 & 1 \end{pmatrix} + V_{NC} \begin{pmatrix} 1 & 0 \\ 0 & 1 \end{pmatrix}. \quad (18.114)$$

We ignore the last two terms appearing in the Hamiltonian due to the fact that they are diagonal and do not affect the relative energy eigenvalues. Therefore, Eq. (18.114) becomes

$$\begin{aligned} H_M &= \frac{\Delta m^2}{4E} \begin{bmatrix} -\cos(2\theta) & \sin(2\theta) \\ \sin(2\theta) & \cos(2\theta) \end{bmatrix} + \frac{1}{2}\sqrt{2} G_F N_e \begin{bmatrix} 1 & 0 \\ 0 & -1 \end{bmatrix} \\ &= \frac{\Delta m^2}{4E} \begin{bmatrix} -(\cos 2\theta - r) & \sin 2\theta \\ \sin 2\theta & (\cos 2\theta - r) \end{bmatrix}, \end{aligned} \quad (18.115)$$

where $r = \frac{2\sqrt{2} G_F N_e E}{\Delta m^2}$. If the mixing angle in the presence of matter is denoted by θ_M and the mass difference squared in matter is denoted by Δm_M^2, then by diagonalizing the matrix, we may write the Hamiltonian part of the oscillation in matter, corresponding to the Hamiltonian in the case of vacuum. Let us start with

$$H_M = \frac{\Delta m_M^2}{4E} \begin{pmatrix} -\cos(2\theta_M) & \sin(2\theta_M) \\ \sin(2\theta_M) & \cos(2\theta_M) \end{pmatrix}.$$

The equation of motion in the matter is given by:

$$i \begin{bmatrix} \dot{\nu}_e(t) \\ \dot{\nu}_\mu(t) \end{bmatrix} = H_M \begin{bmatrix} \nu_e(t) \\ \nu_\mu(t) \end{bmatrix} = \frac{\Delta m_M^2}{4E} \begin{pmatrix} -\cos(2\theta_M) & \sin(2\theta_M) \\ \sin(2\theta_M) & \cos(2\theta_M) \end{pmatrix} \begin{bmatrix} \nu_e(t) \\ \nu_\mu(t) \end{bmatrix}, \quad (18.116)$$

with

$$\begin{aligned} \sin^2(2\theta_M) &= \frac{\sin^2(2\theta)}{\sin^2(2\theta) + (\cos(2\theta) - r)^2}, \\ \Delta m_M^2 &= \Delta m^2 \sqrt{\sin^2(2\theta) + (\cos(2\theta) - r)^2}. \end{aligned} \quad (18.117)$$

The calculated values of the effective masses m_{1M}^2 and m_{2M}^2 are

$$\begin{aligned} m_{1M}^2 &= -\frac{1}{2}\Delta m^2 \sqrt{\sin^2(2\theta) + (\cos(2\theta) - r)^2}, \\ m_{2M}^2 &= \frac{1}{2}\Delta m^2 \sqrt{\sin^2(2\theta) + (\cos(2\theta) - r)^2}. \end{aligned} \quad (18.118)$$

https://doi.org/10.1017/9781108489065.019 Published online by Cambridge University Press

It may be noticed that at zero density $m_{1M}^2 \simeq m_1^2$, and $m_{2M}^2 \simeq m_2^2$ for neutrinos as well as for antineutrinos. It can be clearly seen from Eq. (18.118) that when the density of matter increases from zero to $\cos 2\theta$, the effective mass squared m_{1M}^2 increases for the neutrinos and decreases linearly for the antineutrinos because the effective potential (due to CC interaction) is positive for neutrinos and negative for antineutrinos. Similar observations can be made for m_{2M}^2.

18.3.3 Probability for oscillation in matter

For the two-flavor oscillation scenario in matter, replacing the mixing angle θ(in vacuum) by θ_M(in matter), we may write

$$\begin{aligned}
\begin{pmatrix}\nu_e\\ \nu_\mu\end{pmatrix} &= U(\theta_M)\begin{pmatrix}\nu_1^M\\ \nu_2^M\end{pmatrix} = \begin{pmatrix}\cos\theta_M & \sin\theta_M\\ -\sin\theta_M & \cos\theta_M\end{pmatrix}\begin{pmatrix}\nu_1^M\\ \nu_2^M\end{pmatrix},\\
\Rightarrow \quad |\nu_e(t=0)\rangle &= |\nu_1^M\rangle\cos\theta_M + |\nu_2^M\rangle\sin\theta_M,\\
\text{and} \quad |\nu_\mu(t=0)\rangle &= -|\nu_1^M\rangle\sin\theta_M + |\nu_2^M\rangle\cos\theta_M,
\end{aligned}$$

where ν_1^M and ν_2^M are the mass eigenstates in matter; these are different from the mass eigenstates in vacuum, viz., ν_1 and ν_2.

First, we take the density of matter to be constant and then the solutions will be approximated for matter with varying densities. Following the analogy of Eq. (18.9), we write:

$$\begin{aligned}
|\nu_e(t)\rangle &= |\nu_1^M(t)\rangle\cos\theta_M + |\nu_2^M(t)\rangle\sin\theta_M\\
&= |\nu_1^M\rangle e^{-i\frac{\Delta m_M^2}{4E}t}\cos\theta_M + |\nu_2^M\rangle e^{+i\frac{\Delta m_M^2}{4E}t}\sin\theta_M,\\
\Rightarrow \langle\nu_\mu|\nu_e(t)\rangle &= -\sin\theta_M e^{-i\frac{\Delta m_M^2}{4E}t}\cos\theta_M + \cos\theta_M e^{+i\frac{\Delta m_M^2}{4E}t}\sin\theta_M\\
&= \sin\theta_M\cos\theta_M\left\{2i\sin(\frac{\Delta m_M^2}{4E}t)\right\}. \qquad (18.119)
\end{aligned}$$

The probability that $|\nu(t)\rangle$ (either ν_e or ν_μ) is detected as ν_μ after a time t is given by:

$$\begin{aligned}
P_M(\nu_e\to\nu_\mu) &= |\langle\nu_\mu|\nu_e(t)\rangle|^2\\
&= \left|\sin\theta_M\cos\theta_M\left\{2i\sin(\frac{\Delta m_M^2}{4E}t)\right\}\right|^2\\
&= \sin^2(2\theta_M)\sin^2\left(1.267\Delta m_M^2(eV)\frac{L(\text{km})}{E(\text{GeV})}\right), \qquad (18.120)
\end{aligned}$$

where we used $L = t$ (in natural units). The probability in the matter $P_M(\nu_e \to \nu_\mu)$ is similar to the probability in the vacuum except that here we have replaced θ by θ_M and Δm^2 by Δm_M^2. In the limits of zero matter density, we get back to the case of oscillation in vacuum, that is,

$$\theta_M \to \theta \qquad \text{and} \qquad \Delta m_M^2 \to \Delta m^2.$$

The oscillation probability curve in matter for normal and inverted mass hierarchy are shown in Figure 18.12 for $L = 810$ km, $E = 1 - 6$ GeV, $\Delta m^2 = 2.5 \times 10^{-3}\text{eV}^2$, $\theta = 8.9^\circ$

https://doi.org/10.1017/9781108489065.019 Published online by Cambridge University Press

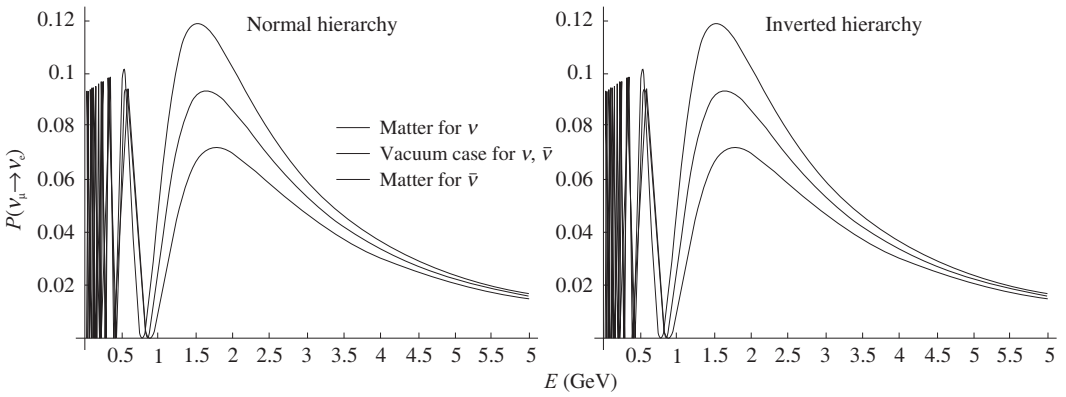

Figure 18.12 Oscillation probability for ν and $\bar{\nu}$ in matter and vacuum as illustration of matter effect. Normal and inverted hierarchy, using NOvA experiment parameters, L = 810 km, E = 1–6GeV, $\Delta m^2 = 2.5 \times 10^{-3}\text{eV}^2$, $\theta = 8.9^\circ$.

18.3.4 Resonance condition and level crossing

In this section, we obtain a mathematical condition for the resonance in terms of the mixing angle in matter and the effective potential. Using the first equation of Eq. (18.117), we obtain:

$$\tan 2\theta_M = \frac{\sin 2\theta}{\cos 2\theta - r}. \tag{18.121}$$

We define $\tan 2\theta_M$ in terms of the vacuum oscillation length(L_v^{osc}), which is defined as the length for which the argument in $\sin^2(L_v \Delta m^2/4E)$ becomes π. This implies $L_v^{\text{osc}} = \frac{4\pi E}{\Delta m^2}$. For the $\nu_e - e^-$ scattering, the interaction length is given by:

$$L_{\text{int}} = \frac{4\pi}{2\sqrt{2}G_F N_e}, \text{then } \frac{L_v^{\text{osc}}}{L_{\text{int}}} = \frac{2\sqrt{2}G_F N_e E}{\Delta m^2} = r. \tag{18.122}$$

Therefore, substituting $r = \frac{L_v^{\text{osc}}}{L_{\text{int}}}$ in Eq. (18.121), we get the mixing angle in terms of the oscillation and the interaction lengths as:

$$\tan 2\theta_M = \frac{L_{\text{int}} \sin 2\theta}{L_{\text{int}} \cos 2\theta - L_v^{\text{osc}}}. \tag{18.123}$$

We define $F = 2\sqrt{2}G_F N_e E$ which is positive in normal matter and $F' = \Delta m^2 \cos(2\theta)$, such that

$$\tan 2\theta_M = \frac{\tan 2\theta}{1 - F/F'}. \tag{18.124}$$

- There is maximal mixing at resonance, that is, the value of effective mixing is $\frac{\pi}{4}$ which leads to the possibility of total transitions between the two flavors, that is, the resonance region is wide enough. This is called the MSW effect.

https://doi.org/10.1017/9781108489065.019 Published online by Cambridge University Press

- Resonance can exist only if $\theta_M < \frac{\pi}{4}$ because $\cos 2\theta_M < 0$, if $\theta_M > \frac{\pi}{4}$. Therefore, neutrino oscillation behaves differently in matter and vacuum, where probability is symmetric under the exchange of $\theta \to \frac{\pi}{2} - \theta$. For antineutrinos, the potential is reversed as there can be a resonance only if $\theta_M > \frac{\pi}{4}$.

In Eq. (18.124), we see that the term $\tan 2\theta_M$ reaches its maximum value for $\theta_M = \frac{\pi}{4}$ or $\tan 2\theta_M = \infty$, or we can say that for maximal mixing, the denominator of Eq. (17.124) becomes equal to zero, that is, $F = F'$ which gives

$$\Delta m^2 \cos 2\theta = 2\sqrt{2} G_F N_e E. \tag{18.125}$$

This condition is known as the MSW resonance condition. When this condition is met, neutrino mixing in matter becomes maximum.

18.4 Neutrino Oscillation: Experimental Status

Neutrino oscillation effects have been observed in several experiments using the neutrinos from following sources:

i) Solar neutrinos: Radiochemical experiments such as Homestake [1018], Gallex/GNO [988], and SAGE [985], as well as time and energy dependent rates from the four phases in Super-Kamiokande [981, 982, 983, 984], the three phases of SNO [989], and BOREXino [986, 987].

ii) Atmospheric neutrinos: Kamiokande [898, 901, 902], SOUDAN [979], MACRO [1019], Super-Kamiokande [903, 980], SNO [1020], MINOS [1021], IceCube [1022], ANTARES [1023].

iii) Accelerator neutrinos: ν_μ and $\bar{\nu}_\mu$ disappearance results from accelerator long baseline experiments MINOS [998] and T2K [1024], and ν_μ, $\bar{\nu}_\mu$ disappearance in NOνA [1025, 628, 1004].

iv) Accelerator neutrinos: Long baseline (LBL) ν_e, $\bar{\nu}_\mu$, ν_τ appearance results from MINOS [999], NOνA [1025, 628], T2K [1026], OPERA [119, 1005, 1006, 1007, 1008], etc.

v) Accelerator neutrinos: Short baseline (SBL) ν_e, $\bar{\nu}_e$ appearance experiments like at MiniBooNE [1027], LSND [1028], etc.

vi) Reactor antineutrinos: $\bar{\nu}_e$ disappearance experiments at Double Chooz [1029], Daya Bay [1030], and RENO [1031].

vii) The energy spectrum of reactor $\bar{\nu}_e$ disappearance at LBL in KamLAND [978].

In the scenario of three neutrino mixing, there are only two independent Δm^2_{ij} say $\Delta m^2_{21} \neq 0$ and $\Delta m^2_{31} \neq 0$. The general convention is that θ_{12}, $\Delta m^2_{21} (> 0)$, and θ_{23}, Δm^2_{31}, respectively represent the parameters which drive the solar (ν_e) and the dominant atmospheric neutrino (ν_μ and $\bar{\nu}_\mu$) oscillations. The parameter θ_{13} is associated with the smallest mixing angle in the PMNS mixing matrix. With the available experimental data, the following parameters are determined, viz. θ_{12}, Δm^2_{21}, θ_{23}, $|\Delta m^2_{31(32)}|$, and θ_{13}.

https://doi.org/10.1017/9781108489065.019 Published online by Cambridge University Press

The value of Δm^2_{ij} are sensitive to different oscillation lengths and neutrino's energy and have been tabulated in Table 18.2. In Table 18.3, we have listed the various neutrino sources like accelerator, reactor, solar, and atmospheric which are sensitive to the different values of oscillation parameters, viz., Δm^2_{ij} and θ_{ij}. The observation of neutrino oscillation in the various experiments imply that neutrinos have mass and there is physics beyond the standard model. The globally best fitted values of oscillation parameters are listed in Table 18.4 and have been taken from PDG [117].

Table 18.2 Δm^2 reach of experiments using various neutrino sources. These experiments have different L and E range.

Neutrinos (baseline)	L(km)	E(GeV)	$\frac{L(\text{km})}{E(\text{GeV})}$	$\Delta m^2_{ij}(\text{eV}^2)$ Reach
Accelerator (short baseline)	1	1	1	1
Reactor (medium baseline)	1	10^{-3}	10^3	10^{-3}
Accelerator (long baseline)	10^3	10	10^2	10^{-2}
Atmospheric	10^4	1	10^4	10^{-4}
Solar	10^8	10^{-3}	10^{11}	10^{-11}

Table 18.3 Neutrino oscillation experiments sensitive to different θ_{ij} and Δm^2_{ij}.

Experiment	Dominant	Important
Solar experiments	θ_{12}	Δm^2_{21}, θ_{13}
Reactor LBL (KamLAND)	Δm^2_{21}	θ_{12}, θ_{13}
Reactor MBL (Daya-Bay, Reno, Double Chooz)	θ_{13}	$\lvert\Delta m^2_{3\ell}\rvert$
Atmospheric Experiments	θ_{23}	$\lvert\Delta m^2_{3\ell}\rvert$, θ_{13}, δ_{CP}
Accelerator LBL ν_μ Disapp (MINOS, NOνA, T2K)	$\lvert\Delta m^2_{3\ell}\rvert$, θ_{23}	
Accelerator LBL ν_e App (MINOS, NOνA, T2K)	δ_{CP}	θ_{13}, θ_{23}, sign$(\Delta m^2_{3\ell})$

The determination of the mixing angles yields at present a maximum allowed CP violation

$$|J_{CP}^{max}| = 0.0329 \pm 0.0009\ (\pm\ 0.0027) \tag{18.126}$$

at 1σ (3σ) for both orderings. The preference of the present data for non-zero δ_{CP} implies a best fit $J_{\text{CP}}^{\text{best}} = -0.032$, which is favored over CP conservation at the $\sim 1.2\sigma$ level.

The oscillation angles are measured to be $\theta_{12} \simeq 34^\circ$, $\theta_{23} \simeq 45^\circ$ and $\theta_{13} \simeq 8^\circ$ [117]. The CP violating phase is not yet measured but recent observations indicate that it may be $\delta^{CP} \simeq -90^\circ$ (maximal CP violation), for example, T2K and NOvA have measured $(P(\nu_\mu \to \nu_e) - P(\bar{\nu}_\mu \to \bar{\nu}_e))$. The T2K experiment hints that δ_{CP} is neither zero nor π [1000]. Recent measurements from T2K [1000] and NOvA [1004] also suggest normal neutrino mass hierarchy.

For details on neutrino oscillation physics, readers are referred to Refs.[1032, 1033].

https://doi.org/10.1017/9781108489065.019 Published online by Cambridge University Press

Table 18.4 The best fit values of the three neutrino oscillation parameters from a global fit of the current neutrino oscillation data. The values (in brackets) correspond to $m_1 < m_2 < m_3$ $(m_3 < m_1 < m_2)$. The definition of Δm^2 used is: $\Delta m^2 = m_3^2 - \frac{m_2^2+m_1^2}{2}$. Thus, $\Delta m^2 = \Delta m^2_{31} - \frac{\Delta m^2_{21}}{2} > 0$, if $m_1 < m_2 < m_3$ and $\Delta m^2 = \Delta m^2_{32} + \frac{\Delta m^2_{21}}{2} < 0$, for $m_3 < m_1 < m_2$.

Parameter	best fit ($\pm 1\sigma$)
$\Delta m^2_{21} 10^{-5}\text{eV}^2$	$7.54^{+0.26}_{-0.22}$
$\lvert\Delta m^2\rvert 10^{-3}\text{eV}^2$	$2.43 \pm 0.06 (2.38 \pm 0.06)$
$\sin^2\theta_{12}$	0.308 ± 0.017
$\sin^2\theta_{23},\ \Delta m^2 > 0$	$0.437^{0.033}_{0.023}$
$\sin^2\theta_{23},\ \Delta m^2 < 0$	$0.455^{0.039}_{0.031}$
$\sin^2\theta_{13},\ \Delta m^2 > 0$	$0.0234^{0.0020}_{0.0019}$
$\sin^2\theta_{13},\ \Delta m^2 < 0$	$0.0240^{0.0019}_{0.0022}$
δ/π (2σ range quoted)	$1.39^{0.38}_{0.27} (1.31^{0.29}_{0.33})$

18.5 Sterile Neutrinos

The standard model (SM) describes the phenomenology of the weak interactions of the three flavors of neutrinos ν_e, ν_μ, and ν_τ, which are considered to be massless, left-handed fermions interacting with matter through the exchange of $W^\pm$ and Z^0 bosons. Moreover, the SM also allows for the existence of massless right-handed neutrinos ν_R which have no interactions with matter and can be called sterile neutrinos. In fact, the idea of non-interacting neutrinos was first conceived by Pontecorvo in 1957 in the context of neutrino reactions with Argon. Subsequently, the discovery of the phenomenon of neutrino oscillations in solar, atmospheric, reactor, and accelerator neutrinos imply that the left-handed neutrinos which interact with matter are not massless. In fact, neutrinos which are the eigenstates of weak interaction Hamiltonian are a coherent mixture of the mass eigenstates of three neutrinos ν_1, ν_2, and ν_3 with very small masses $m_i (i = 1-3)$. The phenomenology of the neutrino oscillations is described satisfactorily in terms of the mass squared differences Δm^2_{ij} $(i, j = 1, 2, 3)$ and the three mixing angles θ_{ij} $(i, j = 1, 2, 3)$. The latest values of Δm^2_{ij} and θ_{ij} are given in Table 18.4. The three flavors of neutrino are also favored by the LEPP data on Z^0 decays and cosmological observations.

However, there are some neutrino oscillation experiments in the last 20 years which have reported anomalous results; the results are not consistent with the three flavor neutrino phenomenology and point towards the existence of additional flavors of neutrinos which are sterile. These sterile neutrinos do not interact with matter in order to be consistent with the LEPP observations but affect the phenomenology of neutrino interactions and neutrino oscillations. These experiments could beare either disappearance experiments with $\nu_\mu(\bar{\nu}_\mu) \to \nu_\mu(\bar{\nu}_\mu)$ and $\nu_e(\bar{\nu}_e) \to \nu_e(\bar{\nu}_e)$ or appearance experiments like: $\nu_\mu(\bar{\nu}_\mu) \to \nu_e(\bar{\nu}_e)$. There exists definite evidence of anomalous results in $\nu_\mu(\bar{\nu}_\mu) \to \nu_e(\bar{\nu}_e)$ and $\bar{\nu}_e \to \bar{\nu}_e$ experiments. In the following, we give a brief account of the experiments which reported anomalous results.

https://doi.org/10.1017/9781108489065.019 Published online by Cambridge University Press

- **LSND experiment [716]:** The liquid scintillator neutrino detector (LSND) was a beam dump experiment at the Los Alamos Meson Physics Facility (LAMPF). It was a very short baseline neutrino (SBN) oscillation experiment: the length was 20 m corresponding to $\frac{E}{L} \sim 1\text{eV}^2$ in which the low energy muon antineutrinos from π-decay and subsequently muon decay were used. The LSND experiment observed an unexpected excess of $\bar{\nu}_e$ events through the inverse β-decay, that is, $\bar{\nu}_e + p \rightarrow n + e^+$, that are interpreted as $\bar{\nu}_\mu \rightarrow \bar{\nu}_e$ oscillations. However, the $\Delta m^2_{12} = 1 - 10\text{eV}^2$ implied by this experiment was too large to be compatible with the other experimental results on Δm^2_{12} and also with our present results on Δm^2_{12} based on the three-flavor analysis of neutrino oscillation experiments. Attempts were made to explain these results by proposing the existence of a neutrino with a fourth flavor as sterile neutrino ν_s and oscillation of the active neutrinos to sterile neutrinos. The experiment also provided limits on the additional mixing parameters Δm^2_{14} and θ_{14}.

- **MiniBooNE experiment [1027]:** The MiniBooNE was an accelerator experiment designed to have the same order of $\frac{L}{E}$ as the LSND experiment to test the anomalous results with the conventional beam of $\nu_\mu(\bar{\nu}_\mu)$ with a broad energy spectrum peaking at 1.25 GeV. The signature of $\nu_e(\bar{\nu}_e)$ respectively in this oscillation experiment was observed by the quasielastic reactions induced by $\nu_e(\bar{\nu}_e)$ which produced charged leptons. An excess of electron-like events was observed in the low energy region around the threshold region of the analysis corresponding to 200–350 MeV. The later experiments with better statistics confirmed the excess of $\nu_e/\bar{\nu}_e$ like events which also suggested the existence of a fourth flavor of sterile neutrinos with Δm^2_{14} in the range of $1 - 5\text{eV}^2$ depending upon a reasonable range of the value of the mixing angle θ_{14}. The $\frac{L}{E}$ corresponding to the MiniBooNE experiment corresponds to a slightly smaller value of $\frac{L}{E}$ compared to the $\frac{L}{E}$ in the LSND experiment but is marginally consistent with it.

- **Gallium anomaly:** A deficit of electron antineutrinos as compared to the predictions was observed in the radiochemical experiments using Gallium (^{71}Ga) targets producing ^{70}Ge in the GALLEX [988] and SAGE [985] experiments. The experiments were being calibrated for solar neutrino experiments and the deficit is known as Gallium anomaly. In the GALLEX experiment, a ^{51}Cr source was used, while in the SAGE experiment, ^{51}Cr as well as ^{37}Ar sources for neutrinos were used. Initially, the deficit was found to be around 15%. These experiments involve nuclei like ^{71}Ge and ^{70}Ge in the initial and the final states leading to some uncertainties in the calculation of weak nuclear cross sections uncertainties from the excited nuclear states. The deficit has been confirmed in later analysis to the 3σ level.

- **Reactor anomaly:** The neutrino oscillation experiments with the reactor antineutrinos at KamLAND [978], Double Chooz [992], Daya Bay [1030], and RENO [1031] have played a very important role in the determination of the neutrino oscillation parameters, specially Δm^2_{21} and θ_{12} and more recently, θ_{13} and Δm^2_{13}. The reactor antineutrino anomaly (RAA) was reported in the context of θ_{13} experiments once the predictions of the antineutrino flux from nuclear reactors were re-evaluated and updated. It refers

https://doi.org/10.1017/9781108489065.019 Published online by Cambridge University Press

to a deficit of antineutrino flux as compared to the predicted flux by about 6% in the antineutrino oscillation experiments operating with 10–100 m from the nuclear reactor and corresponds to a 2.8σ effect. Since the main isotopes contributing to the antineutrino spectra are ^{235}U, ^{238}U, ^{239}Pu, and ^{241}Pu, flux calculations are subject to the theoretical uncertainties arising due to the nuclear structure of these nuclei. The deficit is considered to be a real effect and attempts have been made to explain it in terms of the neutrino oscillations to sterile neutrinos ν_s.

The anomalies in the short baseline experiments at LSND and MiniBooNE and suggestions for the sterile neutrinos have initiated a search for sterile neutrinos in the cosmological observations. The limits on the mixing parameters of the fourth neutrino, that is, Δm^2_{i4} and $|U_{i4}|$ $(i = \mu, \tau)$ are provided by NOMAD [1034], MINOS [1035], SK [1036], and IceCube [1037] experiments. Similarly, limits on the mixing parameters $|U_{e3}|^2 + |U_{e4}|^2$ exist from the SNO experiment [1038]. In the case of astrophysical neutrinos of very high energy from galactic and extra galactic sources, the anomalous events observed by ANITA [1039] collaboration could point to the existence of a fourth flavor of neutrinos. In cosmological observations, quantities like the total number of neutrino species and sum of their masses can be inferred from the study of the cosmic microwave background (CMB), the abundance of light elements in the Big Bang nucleosynthesis (BBN) and large scale structures (LSS) in the universe. While those observations are subject to considerable uncertainties, no definite conclusion can be drawn regarding the existence or nonexistence of additional flavors of neutrinos. If they exist, the mixing parameters like Δm^2_{i4} and θ_{i4} are not consistent with the SBN results [1040].

18.6 Phenomenology of Sterile Neutrinos

The most economical model for sterile neutrinos is to add a single sterile neutrino as a fourth flavor of neutrino ν_s leading to a $3 + 1$ flavor mixing scenario for neutrinos as shown in Figure 18.13. This is called $3 + 1$ flavor instead of four flavor neutrino oscillation, because the fourth flavor neutrino is sterile, that is, it is a non-interacting neutrino while the other three flavors are active and interact with matter. This imposes certain restrictions on the mixing parameters of the fourth flavor ν_s, that is, Δm^2_{i4} and θ_{i4} $(i = e, \mu, \tau, s)$, which are defined through a 4×4 mixing matrix U as:

$$\begin{pmatrix} \nu_e \\ \nu_\mu \\ \nu_\tau \\ \nu_s \end{pmatrix} = \begin{pmatrix} U_{e1} & U_{e2} & U_{e3} & U_{e4} \\ U_{\mu 1} & U_{\mu 2} & U_{\mu 3} & U_{\mu 4} \\ U_{\tau 1} & U_{\tau 2} & U_{\tau 3} & U_{\tau 4} \\ U_{s1} & U_{s2} & U_{s3} & U_{s4} \end{pmatrix} \begin{pmatrix} \nu_1 \\ \nu_2 \\ \nu_3 \\ \nu_4 \end{pmatrix}, \tag{18.127}$$

where ν_i $(i = e, \mu, \tau, s)$ are the flavor states and ν_i $(i = 1, 2, 3, 4)$ are the mass states with mass m_i. This implies that sterile neutrinos are almost the same as the ν_4 mass state. The sterile neutrino flavor state is a mixture of the four mass states. However, three of the mass states must have a very small mixture of sterile neutrinos in order to explain the data in the standard model. This implies the existence of additional splitting Δm^2_{i4} $(i = 1, 2, 3)$ and more parameters to describe the mixing matrix. For example, for a 4×4 matrix, there would be a

https://doi.org/10.1017/9781108489065.019 Published online by Cambridge University Press

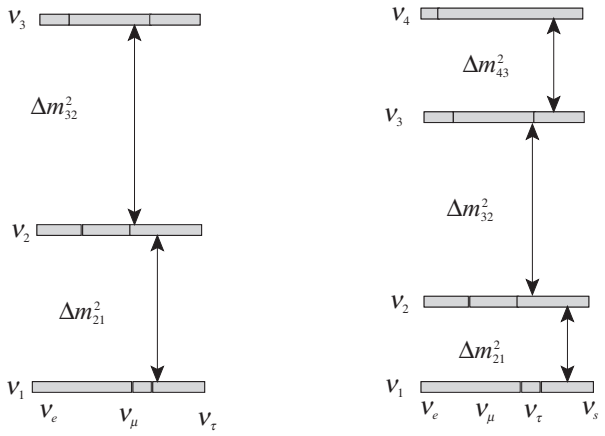

Figure 18.13 Pictorial representation of normal neutrino mass ordering and mixing for the three (left) and four (right) neutrino picture.

total of nine parameters with rotation angles θ_{ij} $(i \neq j)$ and 3 phases. However, in view of the success of the three-flavor oscillation phenomenology, most of the additional parameters will be small and not effective. Moreover, the anomalies in the short baseline experiments indicate that the mass splitting Δm^2_{41} is large, that is, almost ten times the other mass splittings like Δm^2_{21} and Δm^2_{32}. We can therefore work in an approximation where $\Delta m^2_{21} \simeq \Delta m^2_{32} \simeq 0$, the short baseline approximation, in which only one splitting Δm^2_{41}, that is, splitting between the most active and sterile neutrino is important. We also assume that all the neutrinos are Dirac neutrinos. A similar analysis can be done for Majorana neutrinos [1041]. In this approximation:

$$P_{\nu_e \to \nu_e} = 1 - 4(1 - |U_{e4}|^2)|U_{e4}|^2 \sin^2(\Delta^2_{41}), \tag{18.128}$$

$$P_{\nu_\mu \to \nu_\mu} = 1 - 4(1 - |U_{\mu 4}|^2)|U_{\mu 4}|^2 \sin^2(\Delta^2_{41}), \tag{18.129}$$

$$P_{\nu_\mu \to \nu_e} = 4|U_{\mu 4}|^2|U_{e4}|^2 \sin^2(\Delta^2_{41}), \tag{18.130}$$

where L and E are given in kilometers and GeV, or meters and MeV, respectively. Additionally, there are expressions for oscillations probabilities to the τ channel:

$$P_{\nu_\tau \to \nu_\tau} = 1 - 4(1 - |U_{\tau 4}|^2)|U_{\tau 4}|^2 \sin^2(\Delta^2_{41}), \tag{18.131}$$

$$P_{\nu_\tau \to \nu_\mu} = 4|U_{\tau 4}|^2|U_{\mu 4}|^2 \sin^2(\Delta^2_{41}), \tag{18.132}$$

$$P_{\nu_\tau \to \nu_e} = 4|U_{\tau 4}|^2|U_{e4}|^2 \sin^2(\Delta^2_{41}), \tag{18.133}$$

with $\Delta^2_{41} = \frac{1.27\Delta m^2_{41}(eV^2)\ L(Km)}{E(GeV)}$.

18.7 Present and Future Experiments

The present experimental results on the parameters describing sterile neutrino mixing in the $3+1$ flavor model derived from short baseline experiments in the appearance and disappearance mode suggest the presence of sterile neutrinos. However, they do not show the expected

https://doi.org/10.1017/9781108489065.019 Published online by Cambridge University Press

overlapping regions in the parameter space which shows the inadequacy of the 3+1 flavor mixing model. This has led to the consideration of other theoretical models like 3+2 flavor mixing with two sterile neutrinos or 3+1 flavor decay model in which the sterile neutrino decays to invisible particles. On the experimental side, more neutrino oscillation experiments have been proposed to get data with better statistics leading to the determination of mixing parameters with improved precision.

There are a number of experiments proposed to search for sterile neutrinos which have been planned with (anti)neutrinos from radioactive sources, reactors, accelerators and atmospheric neutrinos. In both category of disappearance and appearance experiments [191]. In addition, the experiments planned to directly measure the mass of ν_e $(\bar{\nu}_e)$ neutrinos can also be used to search for the existence of sterile neutrinos.

- Disappearance experiments: Most (anti)neutrino oscillation experiments with radioactive sources and reactors are disappearance type experiments in which radioactive isotopes are artificially produced; these isotopes decay by emitting ν_e or $\bar{\nu}_e$ which are used to perform $\nu_e \rightarrow \nu_e$ or $\bar{\nu}_e \rightarrow \bar{\nu}_e$ type of disappearance experiments. The neutrinos and antineutrinos could have mono energetic or continuous energy spectrum depending upon the decay process. The earlier GALLEX and SAGE were of this type of experiments. Further experiments like SOX at LNGS (Italy), BEST in Baksan, JUNO in China, and ISODAR@KAMLAND in Japan, and ISODAR@JUNO in China are planned with radioactive sources [189].

  All the reactor experiments are disappearance experiments with antineutrino beams. In addition to the earlier reactor experiments, Double CHOOZE, Daya Bay, and RENO which continue with their search for sterile neutrinos, there are new reactor experiments [189]. The present reactor experiments DANSS in Russia has already reported results for $\Delta m^2_{14} = 1.4\ \text{eV}^2$ and $\sin^2(2\theta_{14}) = 0.05$ [1042]. On the other hand, the preliminary results from STEREO at ILL in France [1043] have excluded the parameter space implied by the original reactor antineutrino anomaly (RAA) and Neutrino-4 in Russia [1044] which implies $\Delta m^2_{14} = 7.3\ \text{eV}^2$ and $\sin^2(2\theta_{14}) = 0.39$. Future experiments include NEOS in Korea and SOLID in Belgium.

  The disappearance experiments with ν_μ and $\bar{\nu}_\mu$ are done with accelerator and atmospheric neutrinos in different energy regions. The present experiments of MINOS and NOvA at Fermilab in USA with accelerator neutrinos are upgrading for the sterile neutrino search while the Super-Kamiokande in Japan and IceCube in Antarctica are continuing with their search for sterile neutrinos with atmospheric neutrinos. The short baseline neutrino (SBN) experiment at the Fermilab with three detectors of LArTPC type in the booster neutrino beam (BNB) baseline has an elaborate program for sterile neutrino search in the disappearance mode. The new proposal in the very low energy region of CCM at LANSC [1045], OscSNS at SNS in USA [1046], and JSNS at JPARC [950] are also proposed. All these experiments are designed for the $\nu_\mu \rightarrow \nu_\mu$ and $\bar{\nu}_\mu \rightarrow \bar{\nu}_\mu$ type of disappearance experiments.

https://doi.org/10.1017/9781108489065.019 Published online by Cambridge University Press

- Appearance experiments: The short baseline neutrino (SBN) program at the Fermilab is a dedicated three detector setup designed to search for the sterile neutrino in the ν_e appearance mode in addition to the ν_μ disappearance mode. All the three detectors are liquid argon time projection chambers (LArTPC) called SBND, MicroBooNE, and ICARUS, placed in the BNB baseline in that order with SBND being nearest to the source. The expected signal from a sterile neutrino increases with the baseline and is largest in the ICARUS detector. This is the most ambitious program as it will perform neutrino oscillation experiments in the ν_e appearance as well as the ν_μ disappearance with the same setup and reduce systematics. Other appearance experiments in the kinematic region of LSND have been proposed at the OscSNS facility in USA [1046] and JSNS at JPARC in Japan [950] using neutrino beams from π and K decays at rest.

- Neutrino mass measurement experiments can also be used to search for the presence of sterile neutrinos. These experiments are based on the $\bar{\nu}_e$ mass determination from the energy spectrum from β-decay and electron capture on nuclei. These are (anti)neutrinos of $\nu_e(\bar{\nu}_e)$ type and are a superposition of mass eigen states ν_i $(i = 1,2,3,4)$ weighted by the mixing matrix elements U_{ei}. Therefore, a mixing of the fourth matrix with $m_4 \rightarrow m_i$ $(i = 1,2,3)$ would manifest itself as a kink like signature at the end point of the β decay spectrum. In case of electron capture based on experiments, a detailed analysis of the mass determination of ν_e is required. Experiments like KATRIN and Prospect-8 based on measurements of electrons and experiments like ECHO and Holmes based on ν_e mass determination from electron capture on ^{163}Ho nucleus, using very low energy temperature measurements, are proposed to search for sterile neutrinos.

https://doi.org/10.1017/9781108489065.019 Published online by Cambridge University Press